

## 18 Figures, 0 Appendices, 1 Highlighted Box, 3 Footnotes

### Chapter 6. Leaf Structure and Function

*'Form Follows Function'*, Louis Henri Sullivan (1856-1924), architect

*'Form follows function...has been misunderstood. Form and function should be one, joined in a spiritual union'*, Frank Lloyd Wright (1869-1959), protégé' of Louis Henri Sullivan and architect

Leaves provide the surfaces across which energy and mass are exchanged between plants and the atmosphere. The biochemical constituents that underlie the production and consumption of many trace gases are housed within leaf cells and organelles, requiring that mass in the gaseous state diffuse across leaf surfaces prior to being assimilated or lost from biochemical pathways. Leaves also provide the surfaces upon which much of the solar energy received by an ecosystem is absorbed and they provide the means by which that energy is partitioned into latent and sensible heat loss. The internal environment of a leaf is highly regulated by both structural and functional features. For example, the structural arrangement of leaf cells affects the spatial distribution of photon flux, and the function of stomata affects the diffusive capacity for molecules to cross the external surfaces of the leaf. As indicated in the quotes from two famous architects that we cited above, there is no requisite sequence by which 'form mandates function' or 'function mandates form'; evolutionary modification causes feedback to both anatomy and physiology, forcing both to adjust to each evolutionary increment and maintaining both within an integrated set of constraints that moves species closer to optimal resource use, and ultimately maximizes organism fitness. Leaf form and function must be viewed as highly integrated phenomena, conserved through natural selection.

The integration of leaf form and function is facilitated by cost-benefit constraints associated with the evolutionary process. Leaf size, for example, is determined to large extent by the availability of water required for transpiration and latent heat loss, which in turn is required to maintain a balanced energy budget and keep leaf temperatures near the photosynthetic temperature optimum. Large leaves don't typically exist in perennially hot, dry habitats where latent heat loss is limited, and leaf temperatures often exist close to air temperatures. Leaf thickness is also constrained to certain limits by functional traits. In a

resource-rich environment (e.g., high light, ample water and nitrogen) thick leaves may have an advantage in being able to conduct higher photosynthesis rates. However, at a certain limit, thick leaves will cause a reduction in photon penetration to the point where the cost of producing photosynthetic cells near the bottom of the leaf exceeds their photosynthetic benefits, and diffusive constraints will reduce the supply of  $\text{CO}_2$  to those cells furthest from stomatal pores.

In this chapter we begin our consideration of flux processes at the leaf scale. We will start the chapter by introducing aspects of leaf form, and we will discuss how that form affects the movement of photons,  $\text{CO}_2$  molecules and  $\text{H}_2\text{O}$  molecules through, and within, leaves. We will delay a discussion of the diffusive processes that actually control the flux densities of these molecules until the next chapter. Here, we want to focus on the pathways of flux within the context of leaf anatomy. Near the end of the chapter we will bring into the discussion one aspect of leaf form and function that influences mathematical modeling. That is, the tendency for certain aspects of leaf structure to force non-linearities in the relation between flux and its environmental drivers. We often resolve this complexity by relying on evolutionary tendencies toward optimization as a mathematical 'convenience' with which to linearize otherwise non-linear patterns.

## **6.A Leaf Structure**

Leaves come in different shapes and sizes, ranging from relatively flat, broad structures specialized for capturing solar photons to needle-like structures specialized for low surface-to-volume ratios. In most cases, leaf morphology has evolved in response to selection for maximum photosynthesis rate or minimum transpiration rate, depending on plant growth habit, climatic factors and the availability of growth-limiting resources. In some cases, such as the evolution of thorns, trichomes or fibrous tissues, defense against herbivory has also been an important evolutionary force shaping leaf morphology. Selection for increased defense against herbivory may have been especially important in determining the form of long-lived leaves in resource-poor environments; in these situations, the leaves are exposed to the threat of herbivory for a longer period of time and the resources required to replace eaten leaves are not easily obtained.

An example of the unique relation between leaf size and shape and the advantages provided for  $\text{CO}_2$  and  $\text{H}_2\text{O}$  exchange in specific environments is seen in the desert flora of the

southwestern United States. In a study of the energy budget of desert plants, Gates (1968) noted that leaves tend to be small, and leaf temperatures are closely coupled to air temperatures. He speculated that these two observations were related, and that the small leaf size allowed plants to maximize the exchange of sensible heat with the atmosphere, minimizing the need for evaporative cooling through transpiration, and thus permitting leaf energy budgets to be balanced with low rates of water loss. Ten years later, Gate's theory was modified by Smith (1978), who observed that some desert species have large, flat leaves, and these tend to be the species with greatest access to water; either because they occupy washes or basins and/or possess tap roots that reach deep soil layers. Thus, it appeared that some species adapted to more mesic sites, in this otherwise arid ecosystem, had evolved a type of leaf morphology that favored transpiration and its associated latent heat loss over sensible heat loss. Plants with large leaves and high transpiration rates could maintain leaf temperature close to air temperature (or even more advantageously below air temperature), but by maximizing evaporative heat loss, rather than convective heat loss. The cooler leaf temperatures that are achieved by high rates of transpiration in these species are close to the biochemical optimum for photosynthesis, and thus they permit high rates of CO<sub>2</sub> assimilation.

It would be possible to dedicate an entire chapter to diversity in leaf structure, and discuss the various adaptive outcomes that have occurred given the ecological niches and selective constraints that exist on the earth. We will focus on only one type of leaf to illustrate interactions between structure and function. We will consider the *bifacial leaf*. Bifacial leaves exhibit heterogeneous structures in cross section, with tightly packed cells just beneath the top epidermal surface and loosely packed cells just above the bottom epidermal surface (Figs. 6.1A and 6.1B). The bulk of the cells between the two epidermal layers compose a tissue known as *mesophyll*. Leaf mesophyll cells contain chloroplasts and are specialized for conducting photosynthesis. In many bifacial leaves the mesophyll tissue is organized into two distinct zones: the tightly packed upper zone known as *palisade mesophyll*, and the loosely packed lower zone known as *spongy mesophyll*. In conifer needles, the mesophyll tissue is not differentiated into palisade and spongy layers, but rather occurs as tightly packed cells surrounding a vascular bundle (Fig. 6.1C); a form that results in relatively low surface-to-volume ratios.

The vascular system of the leaf enters through the leaf petiole and is continuous with the vascular system of the plant stem, or tree bole. Vascular bundles in the leaf contain *xylem*, the tissue of water transport, and *phloem*, the tissue of carbon transport (sugars and amino acids). Organic molecules can also be found dissolved in xylem water, but the principal path of carbon transport in the plant is in the form of sugars transported through the phloem. The principal path of water transport in the xylem is from roots to leaves, although water can also be moved among leaves if driven by appropriate water potential gradients. The principal path of carbon transport in the phloem is from leaves, the site of CO<sub>2</sub> assimilation, to growth or storage sinks in the plant; either upward, for the case of transporting sugars to developing tissues at the shoot apex, or downward, for the case of transporting sugars to roots. *Stomata*, pores in the leaf that are bounded by specialized guard cells, can be located either in the upper or lower epidermis, or both, depending on species. Guard cells are typically the only epidermal cells to contain chloroplasts.

## **6.B Convergent evolution as a source of common patterns in leaf structure and function**

We can recognize consistent relations between leaf form and function across broad taxonomic groups of terrestrial plants. We often refer to *plant functional types* (PFTs) as those groups of species that exhibit similar structural and functional attributes. The creation of PFTs is founded on the general recognition that natural selection works independently in different taxonomic lineages to produce convergent, and predictable patterns in the mutually dependent attributes that determine plant form and function (Reich et al. 2003). The attributes by which PFTs are defined can be discrete, such as those that determine the evergreen versus deciduous or woody versus herbaceous growth habits, or continuous, such as those associated with maximum photosynthesis rate or leaf life span.

Natural selection works to modify species attributes in a manner that minimizes the cost and maximizes the benefit of the attribute with regard to plant reproductive fitness. Because many attributes are linked in their effect on plant fitness, evolutionary modification of one attribute is likely to cause a change in the fitness value of a second attribute; and these coupled influences are likely to vary in different environments. Thus, selection often leads to compromises in the value of attributes to plant fitness, a phenomenon we refer to as *adaptive tradeoffs*. As an example, consider the case of plants native to dry ecosystems in which low

stomatal densities on the surface of leaves impose high diffusive resistances (thus limiting water loss), and net primary productivity is, on average, limited by diffusive limitations to CO<sub>2</sub> transport. We know from our previous discussions (see Chapter 4) that plants must allocate nitrogen to leaves in order to produce the enzymes involved in photosynthetic biochemistry and thus, assimilate CO<sub>2</sub>. Nitrogen that is allocated to photosynthetic enzymes in excess of that supported by the diffusive capacity of the leaf will incur a significant cost (in terms of the nitrogen and energy required to construct the enzymes), but with no significant photosynthetic gain. Thus, we can logically invoke a selective tradeoff between a leaf's diffusive potential and its biochemical (photosynthetic) potential. If selection acts to increase the photosynthetic water-use efficiency of a leaf (i.e., the ratio of net CO<sub>2</sub> assimilation rate to transpiration rate), it will come with the negative tradeoff of decreasing the biochemical capacity for CO<sub>2</sub> assimilation. As a second example, consider the case for species native to infertile ecosystems, in which nitrogen or phosphorus availability is likely to limit net primary productivity. If selection acts to maximize photosynthetic phosphorus- or nitrogen-use efficiency (i.e., net CO<sub>2</sub> assimilation rate per unit of nitrogen or phosphorus allocated to photosynthetic enzymes and metabolites), by increasing the diffusive potential of the leaf, and providing a high rate of CO<sub>2</sub> transport to the photosynthetic reactions, it will come with a negative tradeoff of increasing transpiration, and thus decreasing photosynthetic water-use efficiency. We can extend the concept of adaptive tradeoffs to other linked attributes. For example, the photosynthetic limitations inherent in plants from dry or infertile ecosystems will also limit their capacity to sustain high rates of leaf turnover, thus favoring selection for longer leaf life spans. Longer leaf life spans are likely to require higher levels of plant defense which, in turn, is often facilitated by increased leaf toughness, increased production of carbon-rich phenolic compounds and thus more leaf mass per unit of leaf area. Given these patterns, we might expect a tradeoff between leaf life span and leaf CO<sub>2</sub> assimilation rate. Through all of these examples, we find threads of logic that allow us to infer the forces of evolutionary optimization and predict common patterns of covariance in traits associated with leaf form and function.

Inferred relations between leaf form and function are intuitive within the framework of cost-benefit optimization; but how do we know that plant evolution follows our intuition and logic? We must seek supporting observations. We can ask the question: do these generalizations hold up when examined across multiple habitats and ecosystems? Several

studies have been conducted using a broad range of species and it has been shown that even across ecosystem boundaries the structural and functional attributes of leaves are correlated, that they sort out according to PFTs, and they tend to co-vary in patterns that follow the intuitive logic of cost-benefit arguments (Reich et al. 1997, 1999, Wright et al. 2004, Reich et al. 2007; although see Lusk et al. 2008). Species that exhibit the evergreen growth habit, possess woody stems and belong to the gymnosperm taxonomic group tend to have, on average, longer-lived leaves with lower metabolic rates, compared to species that exhibit the deciduous growth habit, possess herbaceous stems and belong to the angiosperm taxonomic group (Fig. 6.2). Species from the ‘slower metabolism’ groups are also native to ecosystems with significant resource limitations to growth (dry, infertile or shaded). The same types of correlations are found in sun and shade leaves. Shade leaves tend to have longer life spans, lower N concentrations and lower rates of metabolism, compared to sun leaves (Ackerly and Bazzaz 1995, Montgomery 2004).

One leaf attribute that has been used as an integrator of form and function is *specific leaf area* (leaf surface area per unit of leaf mass). This attribute is easily measured on dried leaf material, has been reported for many species in many different ecosystems, and appears to be correlated with several functional attributes, such as photosynthesis, transpiration and respiration rates (Wright et al. 2002, 2003, Reich et al. 2003). Thus, SLA can be used as a proxy in many modeling studies to predict rates of leaf-atmosphere exchange. We have provided a more detailed discussion of SLA and its relevance to leaf CO<sub>2</sub> fluxes in Box 6.1.

Taking into account the various observations that have been reported, we can conclude that there are indeed natural patterns of convergent organization within global vegetation that have resulted from past natural selection. These natural patterns can be used as a convenience in the modeling of global surface-atmosphere interactions to produce vegetation assemblages of common flux attributes. For example, we might group together boreal coniferous forests and subalpine coniferous forests as ecosystems with low photosynthetic capacities, compared to deciduous broadleaf forests. Similarly, we might divide a single deciduous, broadleaf forest canopy into two vertical zones with regard to CO<sub>2</sub> and H<sub>2</sub>O fluxes – one with sun leaves, with high flux densities per unit leaf area, and one with shade leaves, with low flux densities per unit leaf area. Recognition of these natural patterns of covariance provides us with a powerful tool in the modeling of ecosystem-atmosphere fluxes.

## 6.C Photon Transport in Leaves

To better understand the photosynthetic assimilation of CO<sub>2</sub> within leaves, we begin with the analogy of a leaf as a photon-gathering 'scaffolding', within which the biochemical apparatus of photosynthesis is embedded. Radiant energy is absorbed by, transmitted through, or reflected from leaves. On average, leaves absorb 40-60% of the total solar energy incident on their surfaces. This value can vary depending on the angle at which solar rays strike the leaf, being closer to 40% for horizontal leaves at low solar angles and closer to 60% for leaves at high solar angles. The absorption by leaves of solar wavelengths in the visible part of the spectrum (i.e., 0.4-0.7 μm), which is also the part of the spectrum utilized in photosynthesis, is much higher; generally being greater than 80% (Fig. 6.3). In the near-infrared part of the spectrum (0.7-1.35 μm), absorption is less than 10%, with most of the energy transmitted through the leaf or reflected from its surface. Beyond the near-infrared part of the spectrum absorption increases again, due to the strong absorption bands of leaf water. Given that the solar energy that strikes the earth is relatively rich in wavelengths from the visible and near-infrared parts of the spectrum (most solar energy at the earth's surface occurs in wavelengths between 0.4-2.5 μm; see Section 2.F), leaves have evolved to maximize their absorption of the visible wavelengths that drive photosynthesis and minimize their absorption of the near-infrared wavelengths that heat the leaf and drive transpiration.

The reflection of incident solar photons that strike leaves includes *diffuse* and *specular* components. Diffuse reflection can occur from both internal and external surfaces; its primary source, however, is from photons that penetrate the leaf and are reflected among the various internal surfaces. Internal reflections cause scattering of the photons, some of which are reflected back across the surface and exit the leaf. Diffuse reflection reaches a maximum when the solar angle is high and solar photons have the greatest opportunity to penetrate the leaf (Fig. 6.4). Specular reflectance occurs through the interaction of photons with the outer leaf surface ('specular' refers to the mirror-like quality of leaf surfaces), and involves reflection along angles that equal the angle of incidence. Specular reflectance is greatest at low solar angles.

The internal reflection of photons that enter a leaf is caused by the sharp refractive discontinuities that occur between intercellular air spaces (refractive index of 1.0) and the surrounding cell walls (refractive index of 1.47 for hydrated cells) (see Walter-Shea and Norman 1991). Generally, the higher the fraction of leaf intercellular air space, the greater the potential

for air-cell wall interfaces, and the stronger the tendency for internal scattering of photons. This is especially obvious when comparing the reflectance patterns for cells near the top versus bottom of a bifacial leaf. When viewed with the human eye, and held perpendicular to a light source, the top surface of a bifacial leaf appears darker in color, whereas the bottom surface appears lighter. This difference is due to greater scattering of photons by the air-cell interfaces of loosely packed cells near the bottom surface. When the air spaces of a bifacial leaf are infiltrated with oil, which approximates the refractive properties of hydrated cell walls, total leaf reflectance decreases by 15-20%.

Specular reflection is caused by the interaction of photons with the outer leaf surfaces. At the macroscopic scale, and ignoring the effects of leaf hairs, leaf surfaces appear to be 'optically smooth'. However, even the smoothest facets of a leaf possess small microscopic irregularities that tend to diffuse some of the intercepted radiation. The specular and diffuse fractions reflected from the outer surfaces of a leaf can be separated on the basis of polarization. Radiation that is reflected in specular fashion is polarized (i.e., oscillations in the radiation field occur in the same direction), whereas diffuse radiation is non-polarized.

The presence of hairs on the leaf surface has an effect on specular reflection; leaf hairs decrease the specular fraction by increasing photon scattering. The capacity of leaf hairs to reflect solar radiation is to some extent dependent on the nature of the hairs themselves. In the desert shrub *Encelia farinosa*, leaves produced during the cool, winter months are covered with a sparse layer of living, fluid-filled hairs, whereas leaves produced during the hot, late-spring are covered with a dense layer of dead, air-filled hairs (Ehleringer and Björkman 1978). Given the strong absorption of infrared wavelengths by water, fluid-filled hairs on the winter leaves would facilitate the *absorption* of infrared radiation during that period when leaf temperatures are coolest. Given the tendency for photon scattering at air-cell interfaces, air-filled hairs on the late-spring leaves would facilitate the *reflection* of infrared radiation during that period when leaf temperatures are high. The dense pubescence layer of *E. farinosa* leaves during the late-spring skews leaf reflectance to favor wavelengths of infrared radiation (0.7-3.0  $\mu\text{m}$ ) relative to photosynthetically-active (0.4-0.7  $\mu\text{m}$ ) radiation (Fig. 6.5). This has a favorable effect on the energy balance of these leaves in their hot, desert environment.

An accurate quantitative understanding of photon scattering is required to assess the photon budget, quantify the amount of photon energy absorbed, and couple photon flux to the exchange

of mass and energy between leaves and the atmosphere. Additionally, the interpretation of remotely-sensed radiometric data acquired with aircraft- or satellite-mounted sensors, which has become so fundamental to our understanding of vegetation-atmosphere interactions, requires knowledge about the reflectance patterns of scattered photons. Theoretically, the angular distribution of the scattered photon flux from a single leaf is described by the *leaf scattering phase function* (Ross 1981):

$$f(\Omega' \rightarrow \Omega; \Omega_L) d\Omega = \frac{dE_L}{dE'_L} \quad (6.1)$$

where  $f(\Omega' \rightarrow \Omega; \Omega_L)$  describes the scattering of photons from the solid angle about direction  $\Omega'$  into direction  $\Omega$  given a leaf surface oriented at direction  $\Omega_L$ . The right-hand side of Equation 6.1 represents the fraction of total incident photon flux from direction  $\Omega'$  (indicated as  $E'_L$ ) that is reflected into direction  $\Omega$  (indicated as  $E_L$ ). Equation 6.1 is presented as a differential equation in order to accommodate reflectance across the entire range of possible leaf viewing angles ( $\Omega$ ); the integration of Equation 6.1 with respect to  $d\Omega$  would provide the total leaf reflectance. Equation 6.1 is a complex statement of a simple concept: *a mathematical function must exist that conserves total photon flux density despite changes in reflected photon flux density when viewed from all possible angles*. Ideally, we would like to understand the first-principles that go into defining  $f(\Omega' \rightarrow \Omega; \Omega_L)$ ; this is key to understanding the controls over photon scattering. Unfortunately, only limited insight exists. We know that  $f(\Omega' \rightarrow \Omega; \Omega_L)$  is determined by the nature of the leaf surface and the internal structure of the leaf, leaf age, pigmentation and leaf hydration status (Gausman 1985); however, quantitative insight into the relationship between these leaf parameters and photon scattering is lacking. Equation 6.1 is often simplified by assuming that the reflected photon flux is entirely diffuse, being isotropically scattered into a solid hemispheric angle normal to the leaf (the *Lambertian assumption*) (see Ross and Nilson 1968, Gutschick and Weigel 1984). This simplification doesn't move us much closer to an understanding of the mechanisms of leaf reflectance, as it perpetuates integral quantities and ignores anisotropic components of the reflected photon stream; which we know exist (see Myneni et al. 1989). It does, however, provide a practical means of using the leaf

scattering phase function, especially to retrieve leaf optical properties from remotely-sensed radiometric data (Privette et al. 1994, Asner and Wessman 1997; also see Pinty and Verstraete 1998). Now, as we proceed with our consideration of how photons are utilized by leaves to energize biochemical processes, we will leave the topic of reflectance and move to the fate of absorbed photons.

Photons that are trapped within the leaf contribute to photosynthesis and other photochemical processes. Leaves have evolved various mechanisms to maximize photon trapping and efficiently deliver photons to the approximately 10 million chloroplasts that occupy each square centimeter of a leaf (Evans 1999). As photons penetrate the waxy cuticular layer of a leaf the first cell they encounter is an epidermal cell. Except for stomatal guard cells, epidermal cells have few chloroplasts and exhibit a convex shape. The convex shape of epidermal cells has the potential to focus a *collimated* photon flux (i.e., a photon flux with parallel incident rays) on underlying mesophyll cells (Fig. 6.6).<sup>2</sup> Epidermal focusing can cause photon flux densities in mesophyll cells that are 10-20 times higher than that incident on the leaf surface; photon focusing creates 'bright' spots in some areas and 'dark' spots in neighboring areas; chloroplasts respond to the bright spots by migrating to them or away from them depending on the intensity of the photon flux (Brugnoli and Björkman 1992, Gorton et al. 1999).

The columnar shape and tight, organized packing of palisade parenchyma cells near the upper surface of bifacial leaves further facilitates the penetration of photons by producing a type of 'light guide' or 'light pipe' that directs collimated rays to the more loosely-organized spongy mesophyll cells near the lower surface. Once in the lower layers photons are scattered by the irregularly-oriented cell wall surfaces, increasing the path length and within-leaf lifetime of the photons, and decreasing the probability that a scattered photon will be transmitted back out of the leaf before it is captured by a chloroplast (Terashima and Saeki 1983). With their effective design for delivering and capturing photons, leaves can be viewed as *light traps* (Fig. 6.7A). One of the more important components of leaf light traps is the inside surface of the lower epidermis; cells of this surface often exhibit a 'whiter' color because of their relative lack of pigmentation and effective capacity to scatter incident photons. As photons traverse a leaf and impinge on the inside surface of the lower epidermis, some are reflected upward, back into the maze of cell surfaces. Light trapping has been shown to increase photon absorption by a factor of 2-5 in a number of plant species (Vogelmann, 1993).

The photon reflections and scattering that occur within a leaf would appear to work against strong stratification in the vertical distribution of the photon flux density; however, steep gradients in PPFD can still occur (Fig. 6.7B). This is because the photosynthetic potential of the leaf decreases from top to bottom, causing more photons to be absorbed near the upper surface compared to the lower surface. The photosynthetic systems of the leaf are distributed such that cells near the upper surface are provisioned with higher densities of chloroplasts, and with each chloroplast containing higher concentrations of photosynthetic enzymes, chlorophyll and light-harvesting proteins. In many ways, the leaf can be viewed as an optimized sink for photons, with photosynthetic systems distributed in a way that maximizes photon utilization. Evidence of optimal photosynthetic distribution is seen in the fact that illumination of a sun-adapted leaf from the lower surface results in lower photosynthesis rates, compared to illumination from the upper surface (Fig. 6.8).

#### **6.D. CO<sub>2</sub> transport in leaves**

The path for CO<sub>2</sub> transport in C<sub>3</sub> leaves begins as molecules diffuse across the leaf surface through the stomatal pores (Figure 6.9A). Once inside the leaf, CO<sub>2</sub> molecules diffuse toward the site of photosynthetic carboxylation, which takes them through the network of intercellular air spaces, across a mesophyll cell wall, across a plasma membrane (cell membrane), through the cytosol of the cell, across the chloroplast membrane and through the stroma of the chloroplast to the active site of Rubisco (Evans and vonCaemmerer 1996, Evans and Loreto 2000). In C<sub>4</sub> leaves, most of the assimilated CO<sub>2</sub> enters the leaf's metabolism (after reacting with H<sub>2</sub>O to form HCO<sub>3</sub><sup>-</sup>) through the enzyme phosphoenolpyruvate (PEP) carboxylase, which is in the cytosol of leaf mesophyll cells. While most models of CO<sub>2</sub> transport in leaves consider the process in one-dimensional space – as a diffusive front that moves from one side of a leaf toward the other – some models have developed the more appropriate three-dimensional framework – considering CO<sub>2</sub> transport as molecules diffuse through discrete pores in the surface, and then disperse in three dimensions into the hemispherical space surrounding the pores (Parkhurst 1994).

Each component of the diffusive pathway in a leaf imposes a resistance to the transport of CO<sub>2</sub>. The principal control over diffusive resistance comes through the variable pore sizes offered by stomata in the leaf's surface(s). With regard to the internal components of the leaf the network of intercellular air spaces imposes a small diffusive resistance compared to that for the

liquid phases of the leaf (e.g., membranes, cytosol and stroma). The most relevant resistive component of the liquid phase is the water-infused channels of the cell walls. The thickness of cell walls is large compared to that of membranes, and aquaporin proteins in the plasma membranes of photosynthetic cells may facilitate CO<sub>2</sub> diffusion (Flexas et al. 2006); thus, cell wall resistance tends to be large and membrane resistance tends to be small. Resistance to CO<sub>2</sub> diffusion through the cytosol of the cell is also likely small. In most leaves chloroplasts are located immediately next to the plasma membrane, making the cytosolic path length inside the cell negligible (Terashima et al. 2006). [In some cases, however, the chloroplasts can migrate to be aligned to the cell wall (parallel to the incoming direct photon beam), increasing the cytosolic diffusive path length; thereby increasing the cytosolic component of leaf resistance (Tholen et al. 2008).] Thus, one of the principal determinants of the internal diffusive resistance to CO<sub>2</sub> transport in leaves is the ratio of mesophyll cell surface area to overall leaf area. The importance of this relation has been long highlighted in the plant physiological literature, extending back to discussion by Park Nobel and his students in the 1970's (e.g., Nobel et al. 1975). The theory underlying diffusive resistances in leaves and their potential to determine leaf-atmosphere flux densities will be discussed in the next chapter.

The intercellular CO<sub>2</sub> concentration within a leaf decreases as a function of distance from the stomatal pores (Fig. 6.9B). The intercellular CO<sub>2</sub> concentration at specific locations within a leaf will be determined by the balance between a 'supply' process (the potential for diffusion to move CO<sub>2</sub> to a specific location within the leaf) and a 'demand' process (the potential for photosynthetic processes to move CO<sub>2</sub> from a specific location within the leaf). The capacity for diffusion to move CO<sub>2</sub> to a specific location is defined by the ratio of the CO<sub>2</sub> concentration gradient (between the ambient atmosphere and the specific location) to the diffusive resistance, and the capacity to remove CO<sub>2</sub> from that location is defined by the biochemical capacity for photosynthesis in the vicinity of the location. Using this type of mass balance logic, isopleths of CO<sub>2</sub> concentration within a leaf can be defined as shown in Figure 6.9B.

Consistent with a common theme we have emphasized in this chapter, the internal structure of leaves has been subjected to evolutionary modification through natural selection; most likely through selection to maximize the CO<sub>2</sub> assimilation rate given a certain capacity for diffusion of CO<sub>2</sub> across the leaf surface. If the availability of water and nitrogen to a plant facilitates high potential CO<sub>2</sub> assimilation rates, those rates will be realized only if the internal structure of the

leaf facilitates high diffusive rates from the stomatal pores to the site of carboxylation. This is best accomplished through high mesophyll surface area ratios (Nobel et al. 1975, Terashima et al. 2001). Once again, structure and function must be highly integrated to facilitate high rates of CO<sub>2</sub> assimilation.

### **6.E Water transport in leaves**

Water moves through leaves according to thermodynamic gradients in water potential (see section 5.D). Leaf thermodynamic gradients take the form of diffusion gradients as water moves from vascular veins to the vicinity of the guard cells, where it evaporates to the atmosphere. Leaf veins provide water to the tissues of the leaf. The hydraulic path from veins through the other tissues of the leaf and into the atmosphere is not well understood. One possible path is for water to diffuse in the vapor phase from the interior air spaces of the leaf, which must exist near 100% relative humidity, to the stomatal pores and out into the atmosphere. However, more evidence exists that leaf veins and the epidermis are hydraulically coupled through the liquid phase, not the vapor phase (Sack and Holbrook 2006). Thus, it is more likely that much of the transpired water moves in liquid phase to the vicinity of the stomatal pore, and then evaporates directly to the atmosphere. Three possible paths exist for this type of water transport: (1) water can flow through the porous cell walls that surround mesophyll or epidermal cells, moving from cell-to-cell (an apoplastic route), (2) water can flow through the internal cytoplasm of mesophyll or epidermal cells, from cell-to-cell, crossing cell membranes via aquaporin proteins (a symplastic route), or (3) water can flow through the plasmodesmatal connections (cytoplasmic connections) between neighboring mesophyll cells, from cell-to-cell (also a symplastic route). Evidence exists to support both apoplastic and symplastic pathways (Westgate and Steudle 1985, Ye et al. 2008), though details of the mechanisms are not yet known. Whatever the exact mechanisms, it is clear that good hydraulic coupling exists between the veins and epidermis, ensuring that changes in the water potential of the entire plant are efficiently communicated to stomatal guard cells. This allows quick response of stomata to changes in the xylem tension of the plant, and thus provides the plant with a means of matching its water loss rate to hydraulic stresses that occur within the plant. In those angiosperms that have been examined, complete rehydration of the epidermis in leaves released from moderate water stress can occur within one to two minutes (Zwieniecki et al. 2007).

The exact path from the minor veins of the leaf to the epidermis requires passage through a layer of cells that surrounds the veins, called the *bundle sheath*. Bundle sheath cells can often span the entire cross-sectional distance from the center of the leaf, where minor veins are located, to the epidermis, thus forming *bundle-sheath extensions* (Figure 6.10). Many bundle sheath cells have a layer of hydrophobic, waxy material in cell walls perpendicular to the veins, which forces most of the water to leave the veins only by crossing the membrane of the bundle-sheath cells, thus entering the cytoplasmic system of the leaf (the symplasm). This causes hydraulic conductivity in the leaf to be sensitive to temperature; membrane viscosity is sensitive to temperature such that at lower temperatures, hydraulic conductivity for H<sub>2</sub>O molecules crossing the membrane decreases (Matzner and Comstock 2001).

Bundle-sheath extensions can facilitate the movement of water from minor veins in the leaf, directly to the epidermis, bypassing most of the mesophyll tissue (Kenzo et al. 2007). This direct path across the leaf may permit effective uncoupling of the hydration states of the mesophyll and epidermis, focusing control over transpiration, and thus latent heat loss from the leaf, on the veins and epidermis. Contrary evidence also exists, however, which supports the existence of a direct evaporation path from mesophyll tissue to the atmosphere (Nanomi and Schulze 1989). There is clearly no consensus at the present time on the exact paths that water takes as it moves through leaves or reason to suspect that such paths are anything but variable among different species or among individual leaves of the same species (see Sack and Tyree 2005, Sack and Holbrook 2006).

Leaf shape can have an influence on boundary layer thickness above the surface of a leaf, and thus leaf temperature and the partitioning of absorbed solar radiation into sensible and latent heat. Leaves with lobes at their margins, or leaves with highly dissected (divided) leaf morphology (e.g., maple leaves or many oak leaves) tend to maintain thinner boundary layers, and thus are more effective at losing sensible heat to the air as wind passes over the surface (Vogel 1970). In an example of form reflecting function, lobed leaves also have a unique hydraulic design (Zwieniecki et al. 2002, 2004). The invaginated leaf margins of lobed leaves are better served by the minor leaf veins of the leaf, compared to leaves with entire margins; in the latter type of leaf, the photosynthetic mesophyll tissue extends further from the central vein network (Sack and Tyree 2005). Thus, in dry habitats, lobed leaves may have a hydraulic

advantage, providing more reliable water supply to the photosynthetic tissues despite low atmospheric humidity or reduced soil moisture.

### 6.F The error of averaging non-linearities in the flux-gradient relation of leaves

Clearly, leaf structure has important effects on the flux densities of CO<sub>2</sub>, H<sub>2</sub>O and solar photons (PPFD). In order to create accurate models of these fluxes we must determine how to mathematically represent the effects of leaf structure on leaf function. Gradients in CO<sub>2</sub>, H<sub>2</sub>O and PPFD affect leaf fluxes in non-linear fashion. For example, we already know that the photosynthetic flux of a leaf responds non-linearly to changes in PPFD and CO<sub>2</sub> concentration (Chapter 4). If we characterize the PPFD or CO<sub>2</sub> concentration within the leaf with average values, and assume that those average values correspond to average photosynthesis rates, we have made the implicit assumption that concentration gradients within the leaf scale linearly with respect to corresponding flux gradients. In mathematical terms, it is assumed that the average result of a function used to relate flux to a driving (independent) variable,  $\overline{f(x)}$ , equals the result when the function is applied to the average of the variable,  $f(\bar{x})$ ; this assumption is valid as long as the relation between the flux and the variable is linear (Fig. 6.11A). For non-linear functions the assumption is not valid; a mathematical property that is often referred to as *Jensen's inequality* (see Ruel and Ayers 1999).<sup>3</sup>

We will explore these principles using the relation between net CO<sub>2</sub> assimilation rate and intercellular CO<sub>2</sub> concentration (the so-called A:c<sub>ci</sub> relationship). As an input to most biochemically-based models of A, the spatially-averaged value for c<sub>ci</sub> is prescribed. This value is then used along with other prescribed values to calculate A. The calculated value for A is assumed to represent the spatial average of all photosynthetic cells distributed across the leaf. However, in the hypothetical case where half the photosynthetic cells are functioning at a c<sub>ci</sub> analogous to  $x(1)$  in the Figure 6.11B, and half are functioning at a c<sub>ci</sub> analogous to  $x(2)$ , the value of A predicted from the average of c<sub>ci</sub> ( $\bar{y}_{app}$  in Fig. 6.11B) will be less than the average of A predicted from independent calculation using each individual value of c<sub>ci</sub> ( $\bar{y}_{true}$  in Fig. 6.11B). This is because the non-linear convexity of the curve allows c<sub>ci</sub> to increase without a proportional increase in A.

In the case of leaf fluxes, averaging across non-linear functions becomes a problem when heterogeneity exists in the distribution of  $c_{ci}$  and PPFD, and the average values for these variables fall within the non-linear portion of the response function. Heterogeneity in  $c_{ci}$  can be caused by vertical gradients in photosynthetic capacity across a leaf, or the presence of anatomical barriers that isolate clusters of cells from one another and prevent lateral integration of diffusive pathways. Vertical gradients in  $c_{ci}$  can develop when diffusive limitations cause the photosynthetic demand for  $CO_2$  to exceed the supply. Thick leaves with well developed palisade and spongy mesophyll, and with stomates only on the lower surface (*hypostomatous*), will develop the largest  $CO_2$  gradients (Fig. 6.12). Hypostomatous leaves are at a diffusive disadvantage in that the palisade mesophyll cells which receive the highest PPFD are the greatest distance from the  $CO_2$  source; leaves with stomates on both surfaces (*amphistomatous*) can more effectively supply  $CO_2$  to the palisade mesophyll tissue. The steep  $CO_2$  concentration gradient across hypostomatous leaves increases their susceptibility to averaging errors.

In addition to heterogeneity along the vertical axis, horizontal heterogeneity is characteristic of many broad-leaved species. In some cases, as discussed above, bundle-sheath extensions stretch from the vascular bundles to the epidermis, potentially facilitating water distribution to the epidermis (Kenzo et al. 2007). The extensions form a diffusive barrier that isolates patches of the leaf into autonomous gas-exchange units, each with their own characteristic stomatal conductance, photosynthesis rate and  $c_{ci}$  (Terashima 1992, Pieruschka et al. 2005); although complete isolation of each gas-exchange unit may not always occur, especially in the face of high photosynthetic rates (Morison and Lawson 2007, Morison et al. 2007). Leaves that are partitioned into lateral units by bundle-sheath extensions are referred to as *heterobaric*. Heterobaric leaves are particularly common in deciduous forest trees from temperate latitudes. Those leaves that lack bundle-sheath extensions, and exhibit lateral continuity in their diffusive pathways, are called *homobaric* (Fig. 6.13). Homobaric leaves are common in evergreen shrubs and trees from warm climates. The fundamental unit of gas-exchange in heterobaric leaves is the isolated patch, or *alveolus*. Stomata of the same alveolus tend to function in a coordinated manner, whereas separate alveoli have the potential to respond independently to environmental signals. In response to low atmospheric humidity or leaf water stress the stomata of some alveoli can be observed to close completely, while others remain open (Terashima et al. 1988). This pattern of heterogeneous distribution in stomatal opening has been

referred to as '*patchy stomatal behavior*'. The occurrence of heterogeneous stomatal patches and the non-linear response of  $A$  to  $c_{ci}$  require that spatially-explicit averaging be applied to the analysis of the  $A:c_{ci}$  relationship (e.g., Meyer and Genty 1998, Kupperts et al. 1999, Mott and Franks 2001, Prytz et al. 2003, Mott and Peak 2007).

The non-linear averaging problem is also relevant to modeling the  $A:PPFD$  relationship. As demonstrated in Figure 6.14, there is an exponential extinction of PPFD across the vertical profile of a leaf. The  $A:PPFD$  curve is also strongly non-linear; thus, when an average PPFD is assumed for a leaf, some of the cells near the upper surface may be at a higher PPFD than those near the lower surface. If the cells near the upper surface are assimilating  $CO_2$  near light saturation, and those near the lower surface are below light saturation, then the same uncertainties in averaging will occur that are illustrated in Figure 6.11B.

In many past models of  $CO_2$  assimilation, averaging uncertainties are acknowledged, but ignored. In the case of  $c_{ci}$ , amphistomatous leaves tend to exhibit across-the-leaf differences in  $CO_2$  mole fraction that are less than  $15 \mu\text{mol mol}^{-1}$  (approximately 6-7% the average  $c_{ci}$  value for a  $C_3$  leaf). Uncertainties in averaging the  $A:c_{ci}$  relationship would be small in these leaves. However, thick, hypostomatous leaves can have  $CO_2$  gradients that measure  $60-70 \mu\text{mol mol}^{-1}$  (approximately 25-30% the average  $c_{ci}$  value for a  $C_3$  leaf). Gradients of this magnitude could cause significant error in a linear averaging of the  $A:c_{ci}$  relationship. Across-the-leaf gradients in PPFD can also be significant (in some cases being  $1500 \mu\text{mol photons m}^{-2} \text{ s}^{-1}$ , or 75% the magnitude of the maximum PPFD received by a leaf).

Returning to our discussion of convergent evolution and cost-benefit optimization as reflected in leaf form and function, we can reconcile non-linearities in the relations between  $A$  and certain driving environmental variables by assuming that phenotypic plasticity forces otherwise non-linear relations into linear form (see Box 6.1). For example, let's consider once again the case of the  $A:PPFD$  relation, which as we have stated is subject to averaging errors when the leaf is considered as a single population of 'average' chloroplasts. These errors are avoided if, in fact, linearity exists between the  $CO_2$  assimilation rate at light saturation ( $A_{\text{max}}$ ) and absorbed PPFD through the vertical profile of the leaf (Fig. 6.14). Thus, as mean PPFD decreases from the top to bottom surfaces, we assume that phenotypic plasticity in the development of leaves allows for differential capacities of leaf layers to utilize photons, and the differences in capacity scale linearly with the differences in mean PPFD. The assumption of

linearity is justified on the basis of evolutionary cost-benefit optimization; leaves are expected to allocate just enough resource (e.g., nitrogen, magnesium, etc.) to the photosynthetic process as is allowed by the available PPFD constraint. As the mean PPFD decreases across the leaf profile, resources will be allocated in progressively lower amounts in proportion to the lower availability of PPFD. This assumption is generally valid for broad-leaved species and for growth in relatively sunny habitats. In such conditions, chloroplasts acclimate to gradients in PPFD, with those near the upper surface exhibiting higher rates of photosynthesis at high PPFD, and those near the lower surface exhibiting higher rates of photosynthesis at low PPFD (Fig. 6.15). This acclimation increases the whole-leaf efficiency by which photons are absorbed and utilized. Chloroplast acclimation is caused, to some extent, by a decline in Rubisco activity through the leaf that parallels the PPFD gradient (Fig. 6.16). With the assumption of linearity between  $A_{\max}$  and PPFD,  $A$  can be modeled as though it is the product of one big chloroplast with a  $V_{\text{cmax}}$  and  $F_{\text{Jmax}}$  that reflect the arithmetic average of the entire leaf. The assumption of linearity depends on the further assumption that chloroplasts are capable of acclimating to the mean PPFD at each leaf layer.

### 6.G. Models with explicit descriptions of leaf gradients

As an alternative to the ‘big chloroplast’ simplification, some researchers have developed vertically-explicit models to accommodate the variation in PPFD across a leaf and its effects on  $A$  (e.g., Terashima and Saeki 1983). These types of models involve partitioning the leaf into successive vertical layers, which are homogenous in the horizontal plane, but heterogeneous in the vertical plane. Using a ‘photon accounting’ approach, and the assumption of conservation of photons, the cumulative photon absorption for vertical layers between the leaf’s surface and depth  $z$  can be represented as:

$$a_z = [1 - r_o - t_z + r_{1z}(1 - \beta - \tau)] I_t \quad (6.2)$$

where  $a_z$  is the total photon flux absorbed between the surface of the leaf and depth  $z$ ,  $r_o$  is surface reflectance (fraction of incident PPFD that is reflected off of the leaf surface),  $t_z$  is the transmittance (fraction of incident PPFD that is transmitted) of all layers between the surface and depth  $z$ ,  $r_{1z}$  is the reflectance (referenced to incident PPFD at the leaf surface) that is reflected

upward from all layers below depth  $z$ ,  $\beta$  is the fraction of  $r_{1z}$  that is reflected back downward before traversing depth  $z$ ,  $\tau$  is the fraction of  $r_{1z}$  that is transmitted back out the upper surface of the leaf, and  $I_t$  is the total (direct plus diffuse) PPFD incident on the surface of the leaf (Fig. 6.17).<sup>2</sup> Higher-order reflections, beyond  $r_{1z}$ , are ignored. After parameterization for the various reflectance and transmittance values,  $A$  for each successive vertical layer, and its response to absorbed PPFD, can be modeled according to the equations described in Chapter 4. The primary inputs for the photosynthesis model of each layer would be the absorbed photon flux and the maximum rates of photosynthetic electron transport ( $F_{J_{\max}}$ ) and RuBP carboxylation ( $V_{c_{\max}}$ ) adjusted for acclimation to the intra-leaf gradient in PPFD. The value of  $A$  for the entire leaf is then calculated as the cumulative sum of  $A$  for all layers.

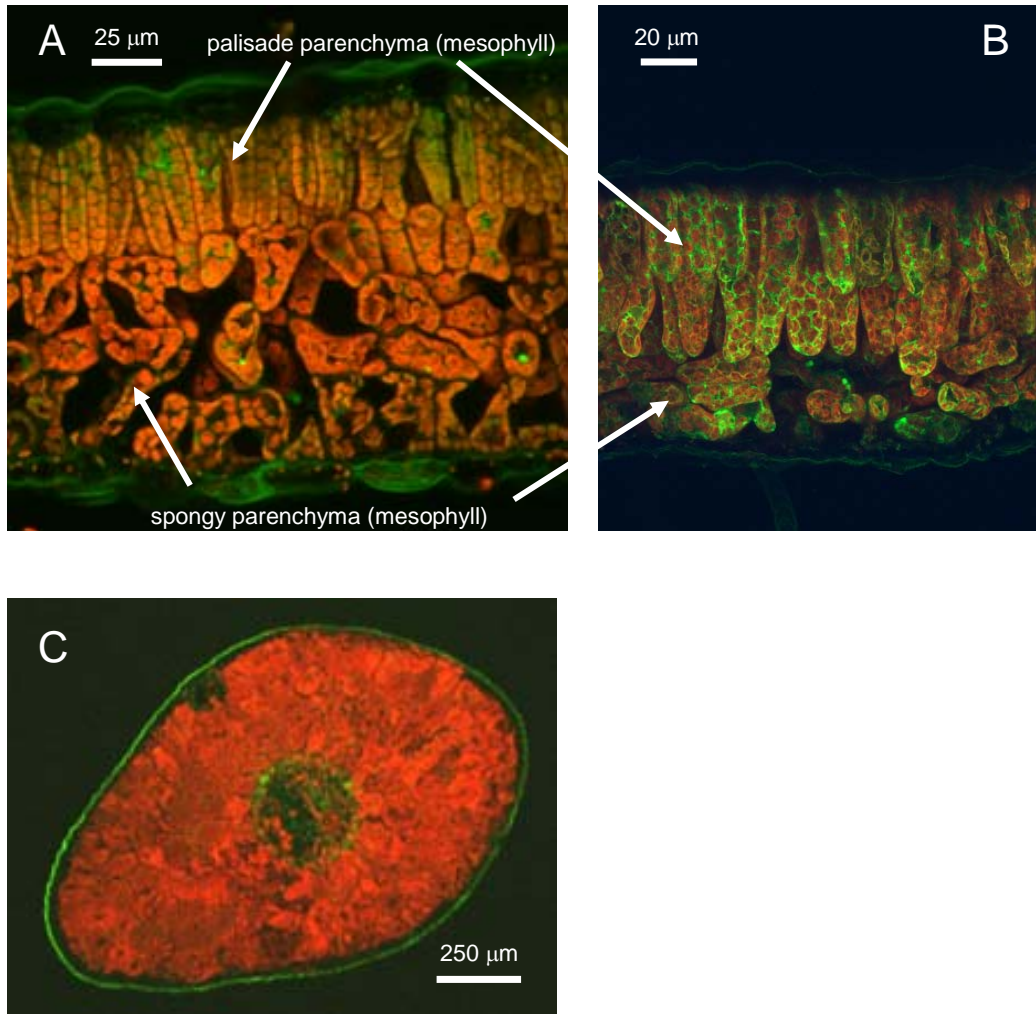


**Figure 6.1.** **A.** Confocal microscope picture of an oak leaf (*Quercus ilex*) showing yellow-fluorescent chloroplasts within a single layer of tightly-packed palisade mesophyll cells just beneath the upper epidermis and loosely-packed spongy mesophyll cells, with large, interspersed air channels, just above the lower epidermis. **B.** Two palisade mesophyll layers above spongy mesophyll tissue in a poplar leaf (*Populus trichocarpa*). **C.** Tightly-packed mesophyll cells surrounding the vascular bundle in a Norway spruce needle (*Picea abies*). Micrographs courtesy of Professor Joerg-Peter Schnitzler (Karlsruhe Forschungszentrum, Garmisch, Germany).

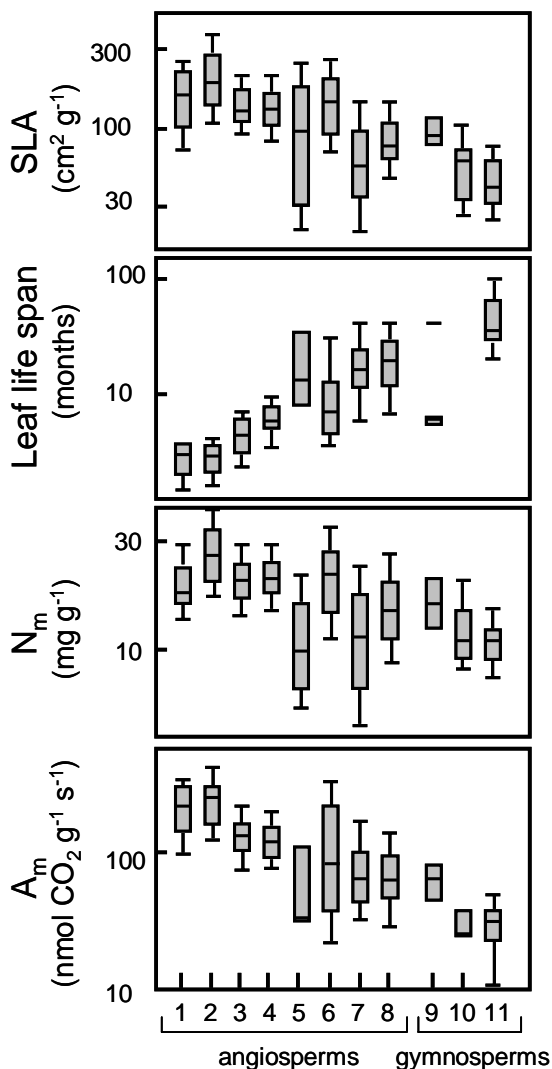


**Figure 6.2.** Leaf structural and functional attributes for 11 plant functional types (PFTs). Plant functional types are: (1) deciduous grasses, (2) deciduous herbs, (3) deciduous shrubs, (4) deciduous trees, (5) evergreen grasses, (6) evergreen herbs, (7) evergreen shrubs, (8) evergreen trees, (9) deciduous trees, (10) evergreen shrubs, and (11) evergreen trees. There are clear trends toward less specific leaf area (SLA) (i.e., thicker leaves), longer leaf life spans, lower leaf nitrogen concentrations per unit mass ( $N_m$ ), and lower photosynthetic capacities per unit leaf mass ( $A_m$ ) in gymnosperms compared to angiosperms, trees compared to shrubs, grasses and herbs, and in evergreen plants compared to deciduous plants. (Redrawn from Reich et al. 2007).

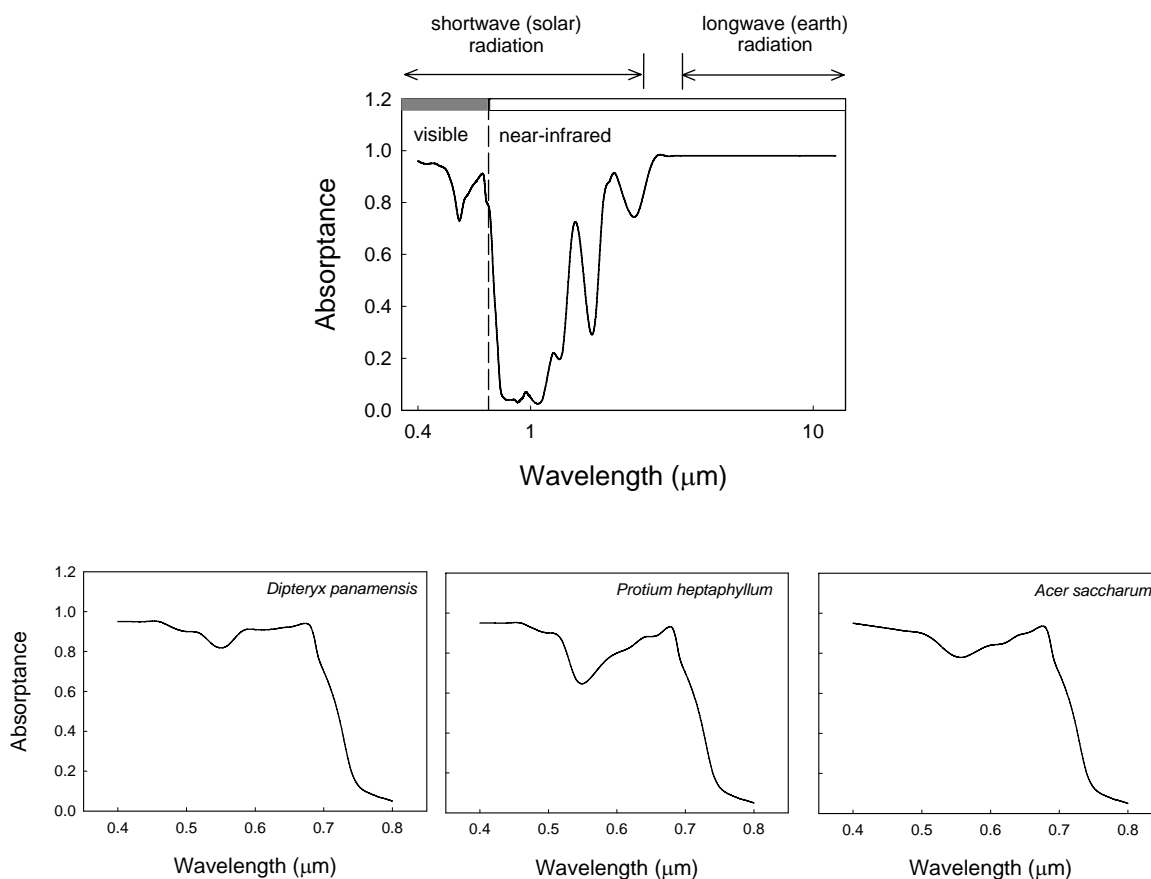


**Figure 6.3. Upper.** The spectral distribution of solar and earth radiation absorption by a cottonwood leaf (*Populus deltoides*). Absorbance is the fraction of incident radiation at each wavelength that is absorbed. A high fraction of the incident visible radiation is absorbed, whereas a considerably lower fraction of near-infrared radiation is absorbed. The visible and near-infrared parts of the spectrum are characteristic of shortwave, solar radiation. Absorption of longwave, earth-emitted radiation by leaves is also high. Redrawn from Gates (1980).

**Lower.** Absorption spectra of three representative leaves in the visible part of the spectrum, showing that absorbance is higher in the red and blue parts of the spectrum and lower in the green part of the spectrum. The absorption spectra also show the decline in absorbance in the initial wavelengths of the near-infrared part of the spectrum. *D. panamensis* and *P. heptaphyllum* are tropical forest tree species. *A. saccharum* is sugar maple, a temperate, deciduous forest species. Redrawn from Poorter et al. (1995), Roberts et al. (1998) and Carter et al. (2000), respectively.

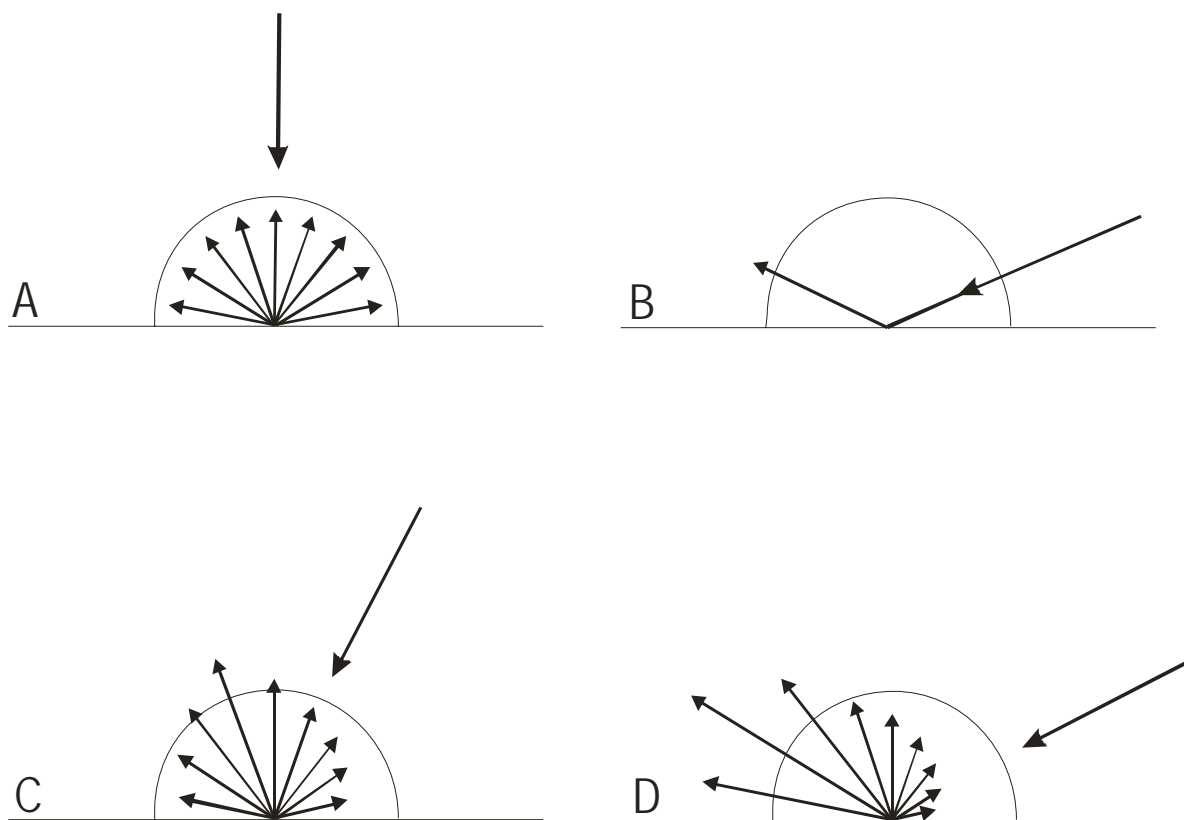


**Figure 6.4.** **A.** The hemispherical pattern of diffuse (or Lambertian) reflectance. **B.** Specular (or non-Lambertian) reflectance. **C.** Combined diffuse and specular reflectance when the angle of solar incidence is high. **D.** Combined diffuse and specular reflectance when the angle of solar incidence is low. Adapted from Gates (1980).

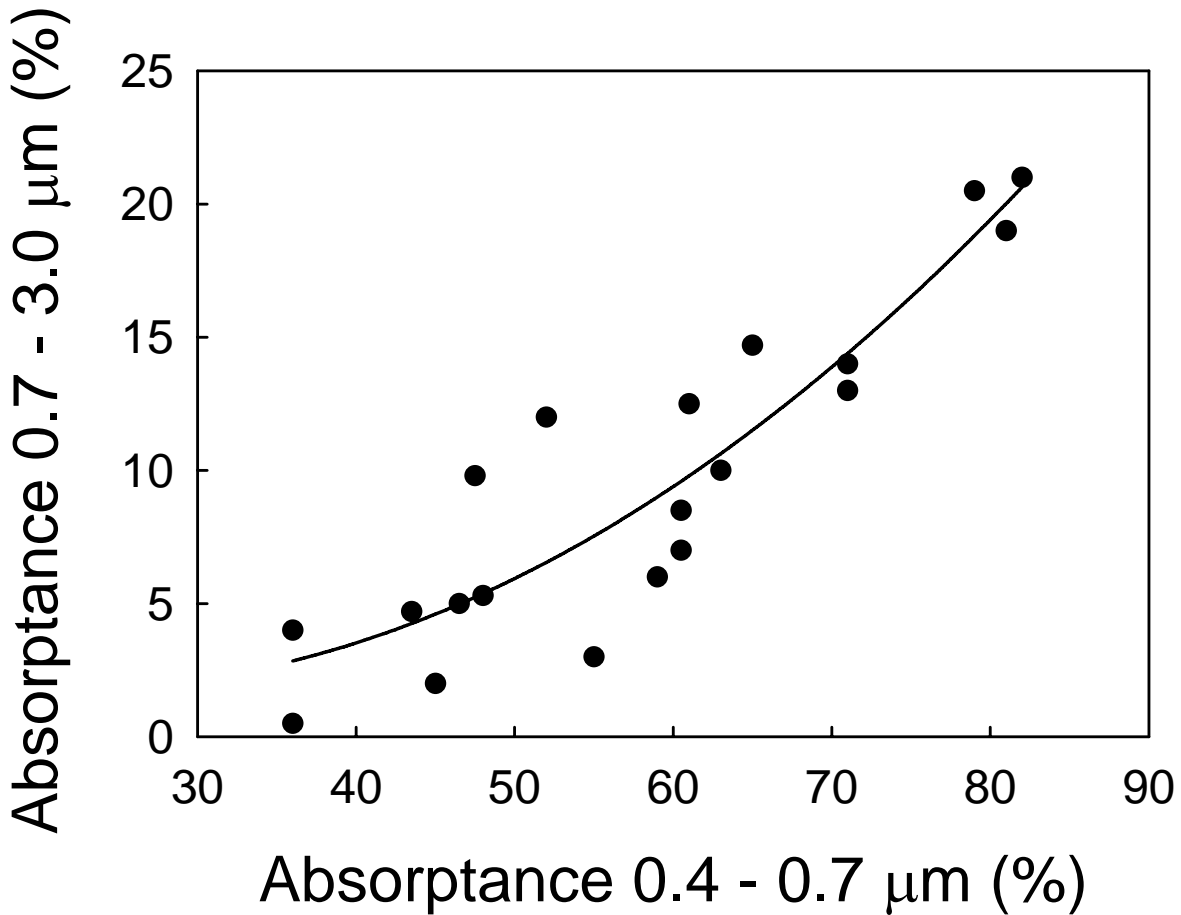


**Figure 6.5.** Relationship between the absorptance of photosynthetically-active radiation (0.4-0.7  $\mu\text{m}$ ) and infrared radiation (0.7-3.0  $\mu\text{m}$ ) in leaves of *Encelia farinosa* (desert brittlebush). The points represent measurements taken at different times of the year. As the seasonal climate becomes hotter and drier absorptance of infrared radiation decreases more than absorptance of photosynthetically-active radiation. Redrawn from Ehleringer and Björkman (1978).

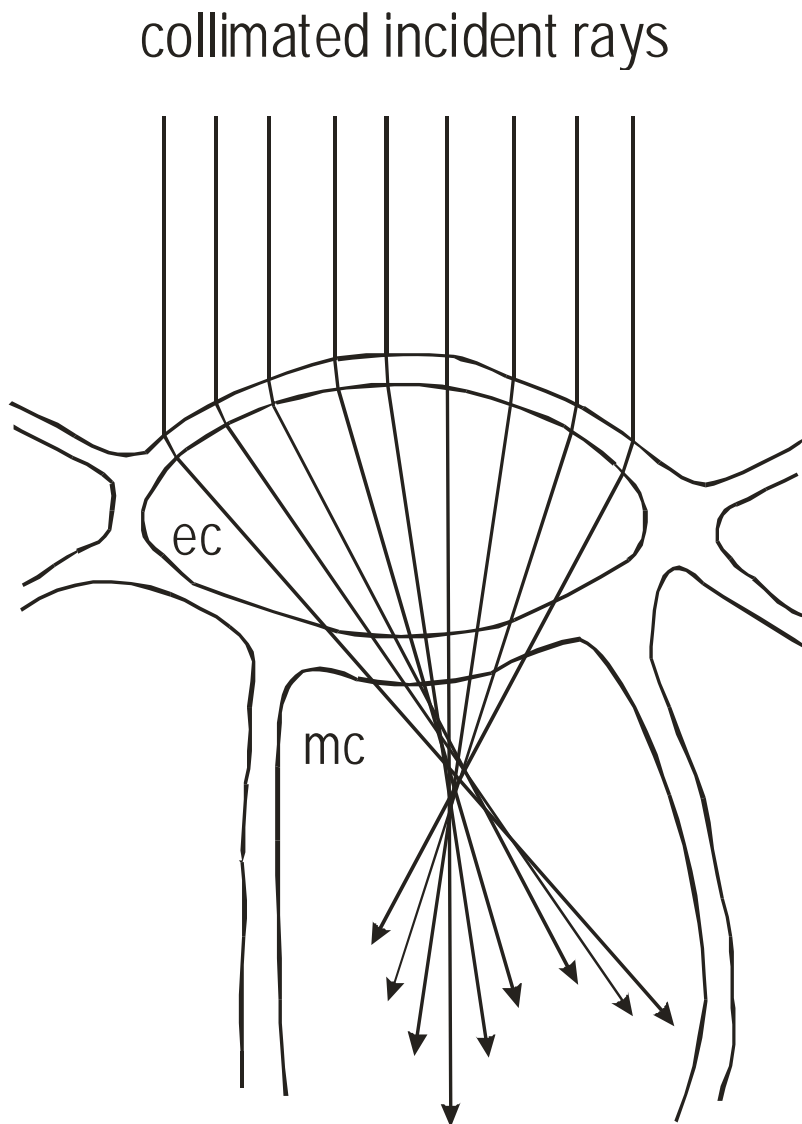


**Figure 6.6.** The focusing of collimated solar rays by an epidermal cell (ec) of the adaxial surface of a leaf to a focal region in the underlying palisade mesophyll cell (mc). Adapted from Vogelmann et al. (1989).

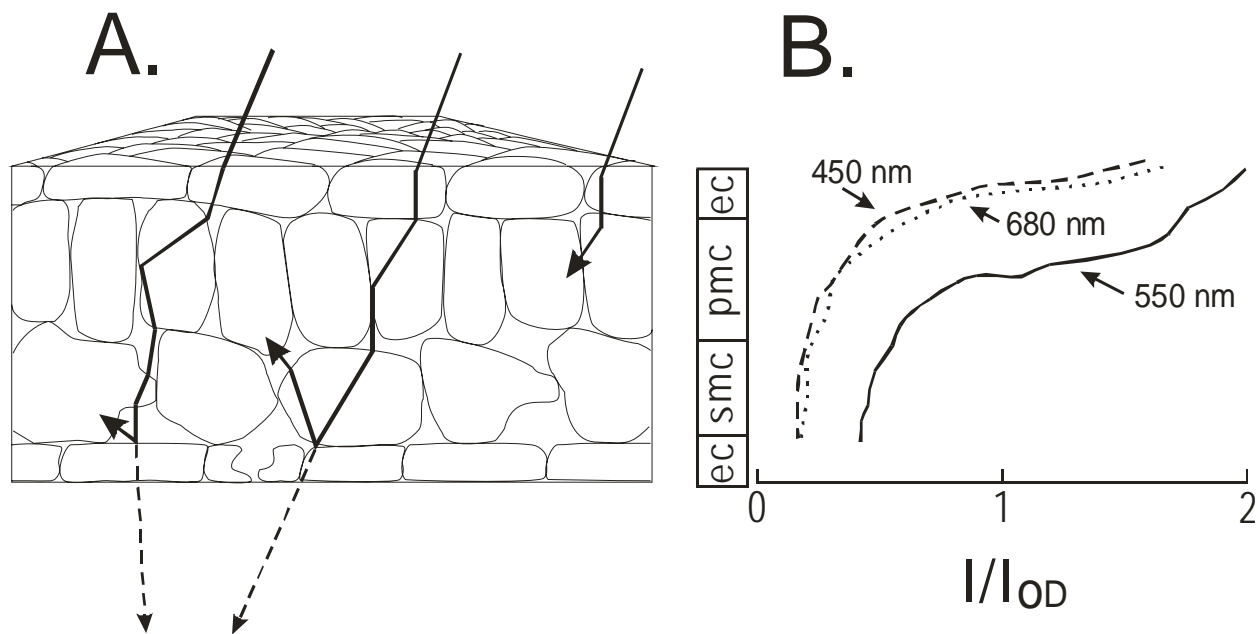


**Figure 6.7.** **A.** Schematic of a leaf cross section illustrating light trapping through multiple reflections from cell surfaces. In this case, the paths for three different, hypothetical photons are presented. The dashed arrows show possible escape routes through the lower epidermis. **B.** Photosynthetic photon flux density (PPFD) profiles for three different wavelengths expressed as the ratio of measured direct beam PPFD to incident direct beam PPFD ( $I/I_{0D}$ ) for a leaf of *Medicago sativa*. PPFD at different points along the vertical profile was measured with the use of a microscopic photon flux sensor that was progressively pushed through the leaf. Note that the PPFD within the leaf can be higher than that incident on the surface due to photon focusing. Also note the strong extinction of photosynthetically active photons in the blue (0.45  $\mu\text{m}$ ) and red (0.68  $\mu\text{m}$ ) wavelengths in the region of the palisade mesophyll. ec = epidermal cells, pmc = palisade mesophyll cells, smc = spongy mesophyll cells. Adapted from Vogelmann et al. (1989).

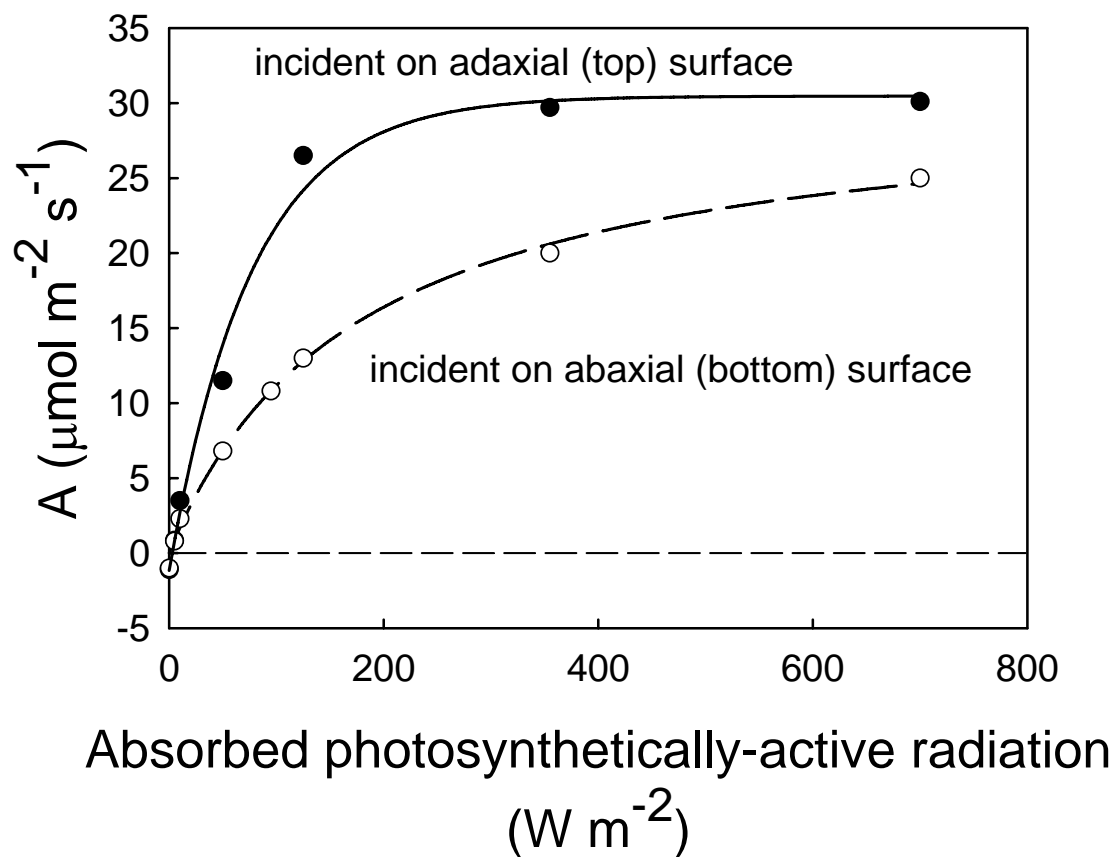


**Figure 6.8.** The response of net  $CO_2$  assimilation rate ( $A$ ) to absorbed photosynthetically active radiation in a leaf of *Syringa vulgaris* when light is provided to the adaxial (top) surface or the abaxial (bottom) surface. Note that the sharpest transition from light-limited to light-saturation occurs when the light energy enters from the adaxial surface. In this case, all chloroplasts became light saturated at approximately the same incident light intensity because the intra-leaf light gradient parallels the pattern of palisade and spongy mesophyll acclimation. When illuminated from the abaxial surface, the spongy mesophyll chloroplasts saturate at a relatively low incident light intensity and the palisade mesophyll chloroplasts saturate at a higher incident light intensity, resulting in a more gradual transition to saturation. Redrawn from Oya and Laisk (1976) and Terashima and Hikosaka (1995).

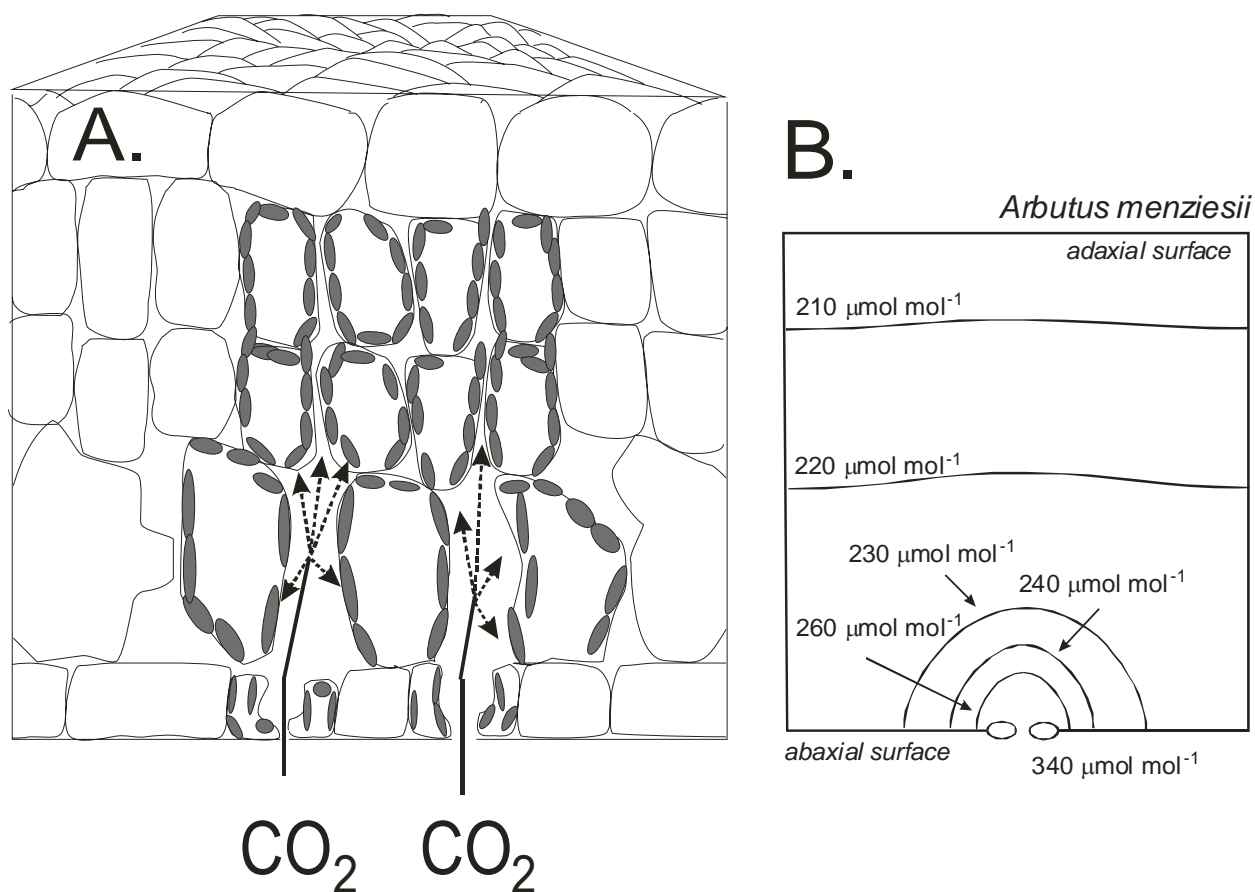


**Figure 6.9.** **A.** Representative diffusion paths for CO<sub>2</sub> crossing the stomatal pores of a hypostomatous leaf. The arrangement of chloroplasts at the periphery of the cytosol minimizes the diffusion path length within the cell. Most of the internal conductance to diffusion of CO<sub>2</sub> is determined by the mesophyll cell surface area and the surface area of chloroplasts pressed against the internal cell surface. **B.** Isopleths of modeled intercellular CO<sub>2</sub> mole fraction using a three-dimensional anatomical model of a leaf of *Arbutus menziesii*, a thick-leaved species in the Ericaceae, showing progressive depletion of CO<sub>2</sub> as the diffusion pathlength from the stomatal pore increases. (Redrawn from Parkhurst 1994).

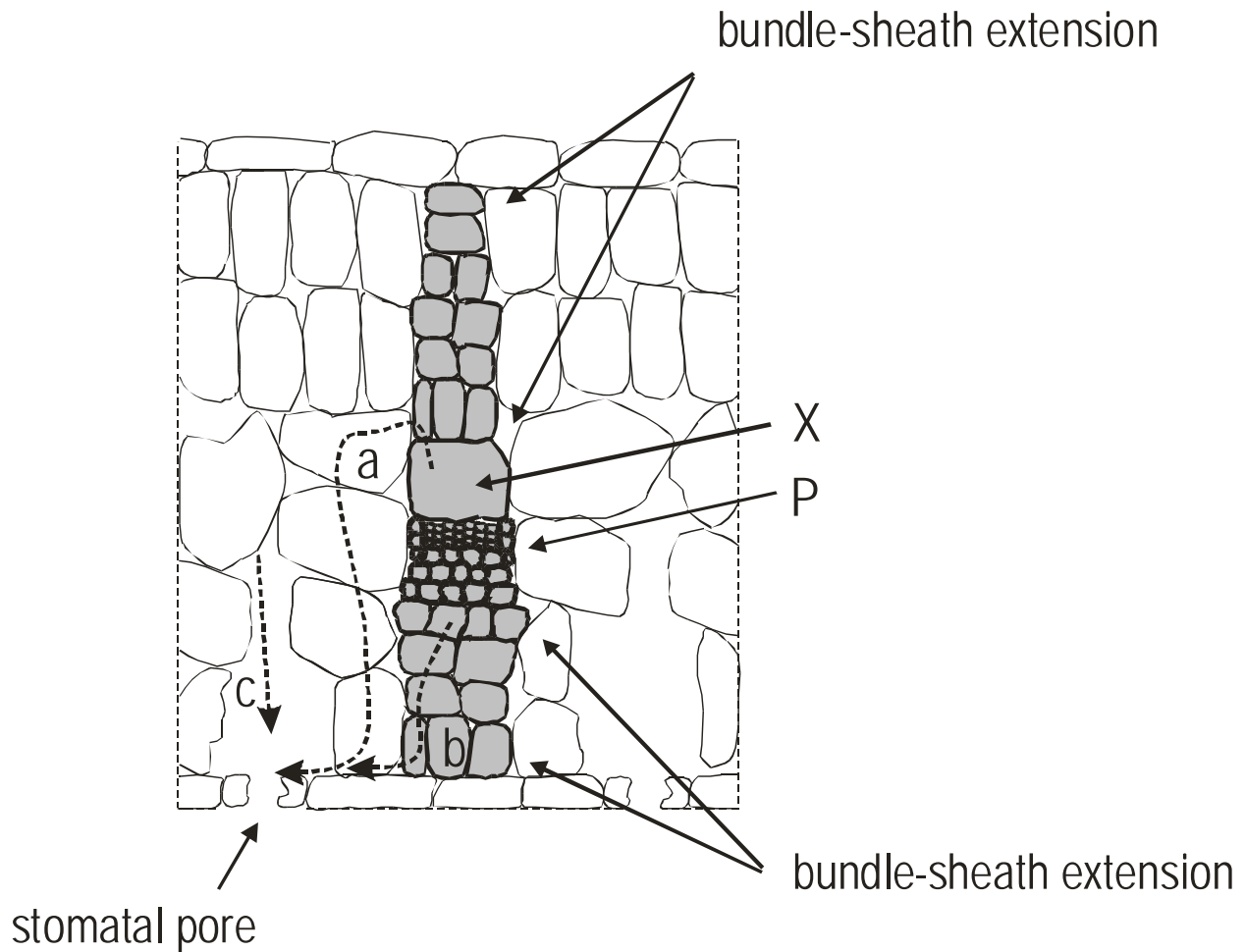


**Figure 6.10.** Possible paths for liquid water to take as it moves through the leaf in response to water potential gradients and arrives at the stomatal pore where it can exit the leaf in the vapor phase. In paths a and b, the water moves symplastically (through cells) from the xylem (X), through bundle-sheath extensions, to the stomatal pore in the epidermis. This path requires liquid water to cross membranes or travel through protein pores in the membrane known as aquaporins. Membrane hydraulic conductivity is temperature sensitive, with viscosity increasing and conductivity decreasing at low temperatures. In path c, water evaporates from the outer cell wall of mesophyll cells and diffuses in vapor phase to the stomatal pore. P = phloem

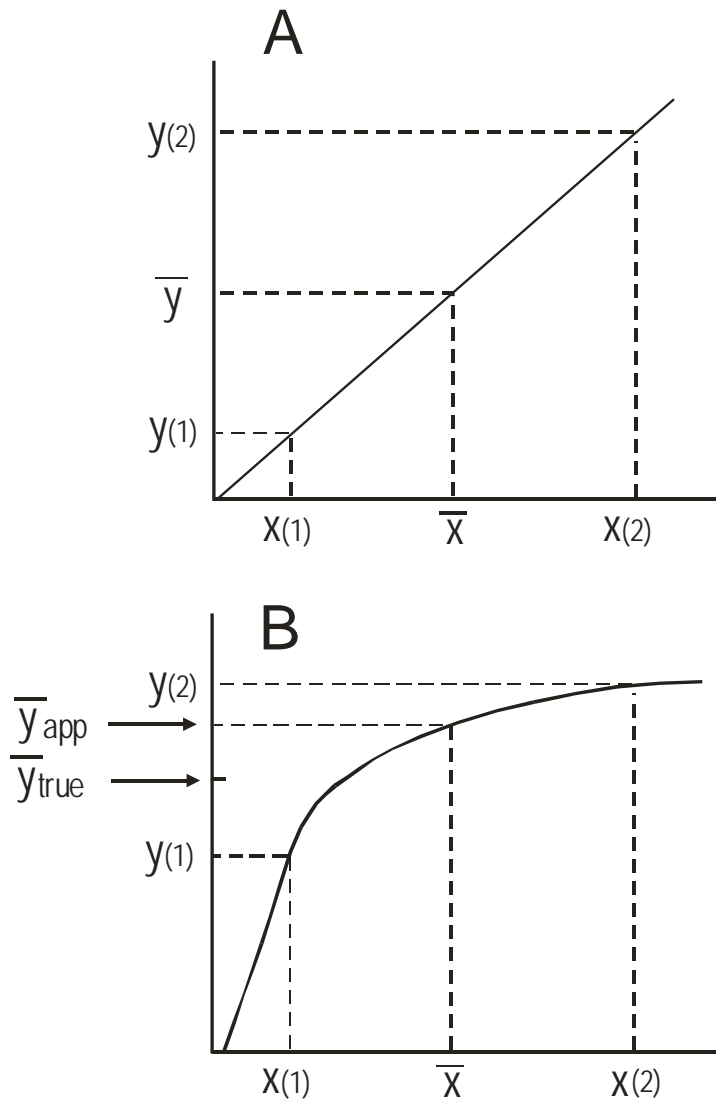


**Figure 6.11. A.** The concept of linear proportionality is illustrated with respect to determining the mean value for a dependent variable from the mean value of an independent variable. **B.** Convex non-linear relationships cause the apparent mean ( $\bar{y}_{\text{app}}$ ) to be an overestimate of the true mean ( $\bar{y}_{\text{true}}$ ).

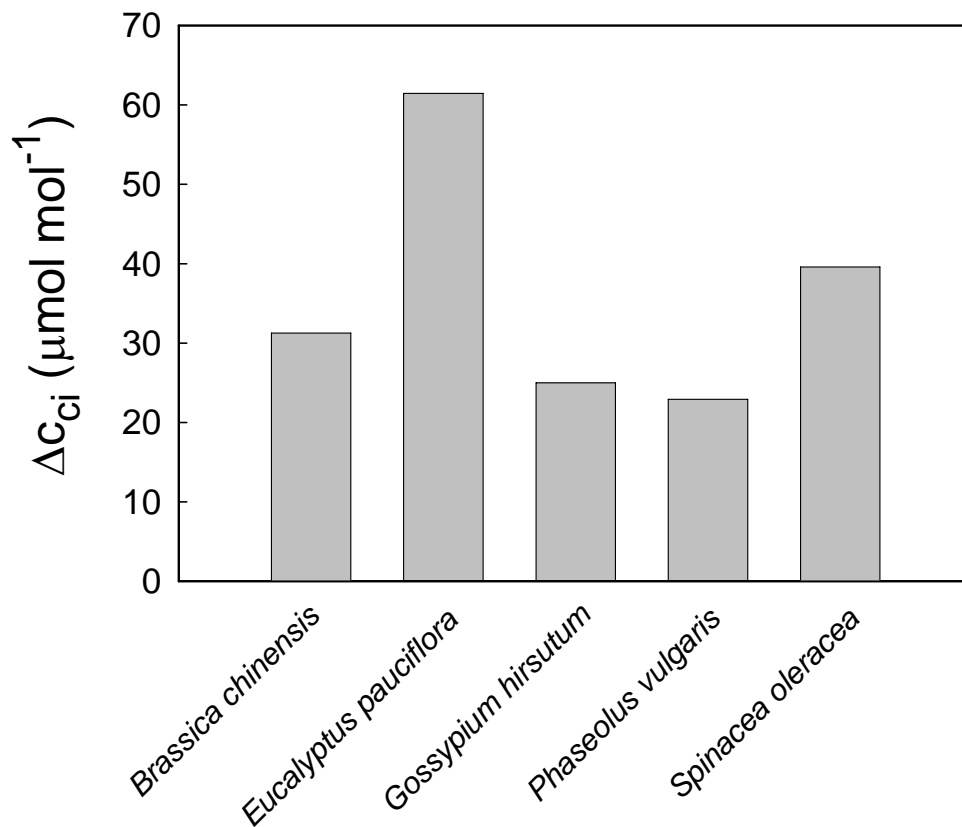


**Figure 6.12.** The difference in CO<sub>2</sub> mole fraction ( $\Delta c_{ci}$ ) across the cross-sectional distance of amphistomatous leaves from different species measured when normal ambient CO<sub>2</sub> concentration was provided to the lower leaf surface with one leaf cuvette, and the concentration at the adaxial leaf surface was measured with a different cuvette. Thus, normally amphistomatous leaves were forced to behave like hypostomatous leaves. (It is not possible to conduct this type of measurement with hypostomatous leaves.) Note the relatively large  $\Delta c_{ci}$  for the thick-leaved *Eucalyptus* species. Adapted from Parkhurst et al. (1988).

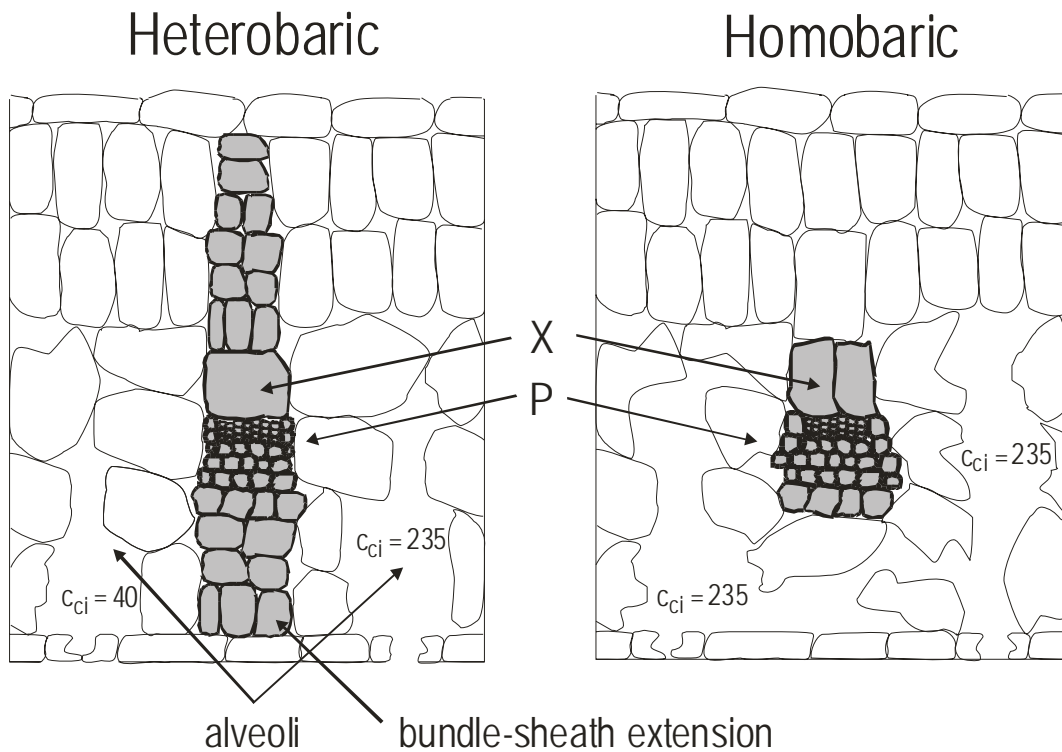


**Figure 6.13.** Cross-sectional depiction of heterobaric and homobaric leaves (see text for details of these terms). Bundle-sheath extensions extend from the vascular bundle to the upper and lower epidermi of the heterobaric leaf. The extensions divide the leaf into separate alveolar units. In the leaf on the left, the stomate that serves the left alveoli is closed and the  $c_{ci}$  exists near the CO<sub>2</sub> compensation point; the open stomate that serves the alveolus on the right maintains the  $c_{ci}$  at 235  $\mu\text{mol mol}^{-1}$ ). X = xylem, P = phloem.

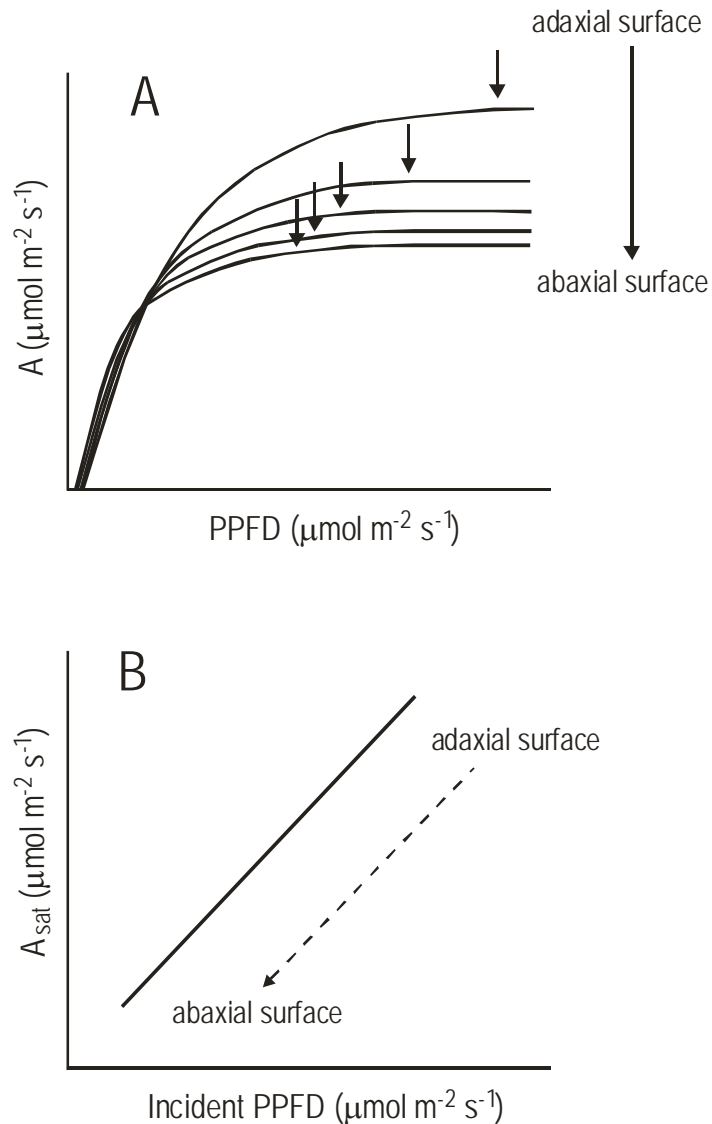


**Figure 6.14.** **A.** The A:PPFD relationship for hypothetical mesophyll cells at different layers within a leaf. The arrows represent the point of incipient PPFD saturation for A, as well as the PPFD that is incident at each respective layer. Thus, as the incident PPFD decreases through the leaf, A remains PPFD-saturated. **B.** The relationship between PPFD-saturated A ( $A_{\text{sat}}$ ) at different hypothetical layers within a leaf and the PPFD that is incident at each respective layer. Note that as a result of the progressive acclimation of cells to lower incident PPFD (as illustrated in panel A), the A:PPFD relationship is linear across the leaf.

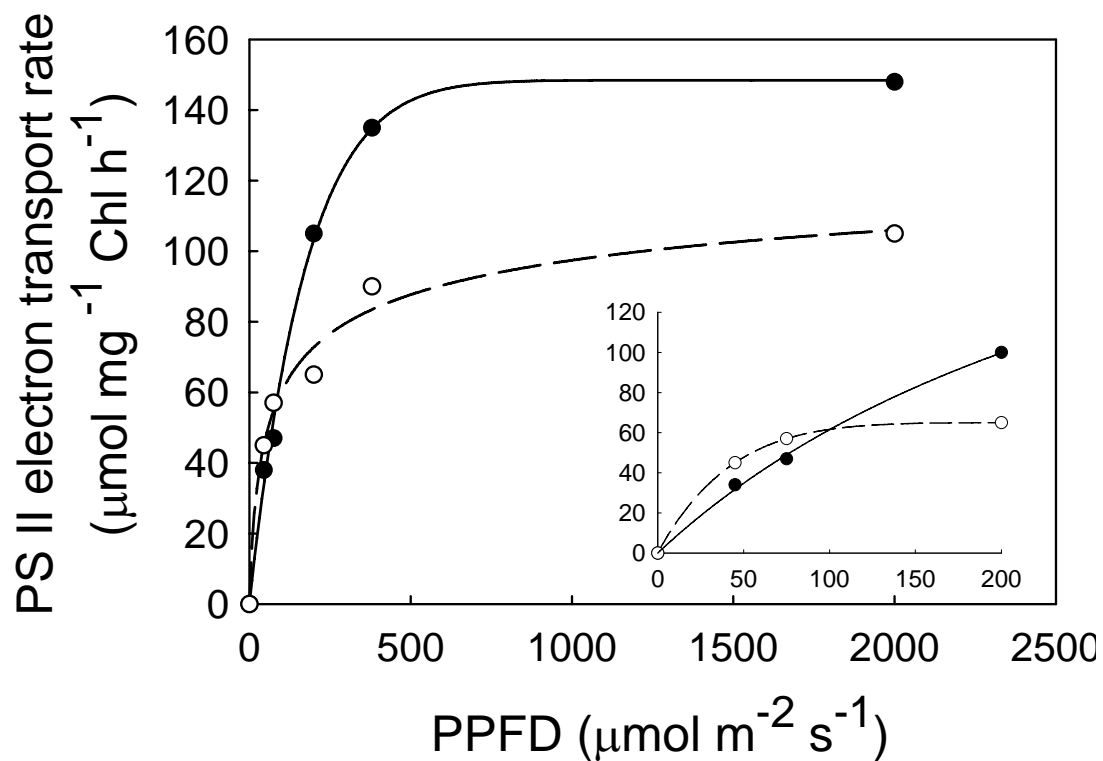


**Figure 6.15.** The response of photosystem II electron transport rate to PPFD in isolated cells from palisade mesophyll tissue or spongy mesophyll tissue of *Camilla japonica* leaves. **Inset:** The same response but for a limited range of low PPFD. Redrawn from Terashima and Inoue (1984).

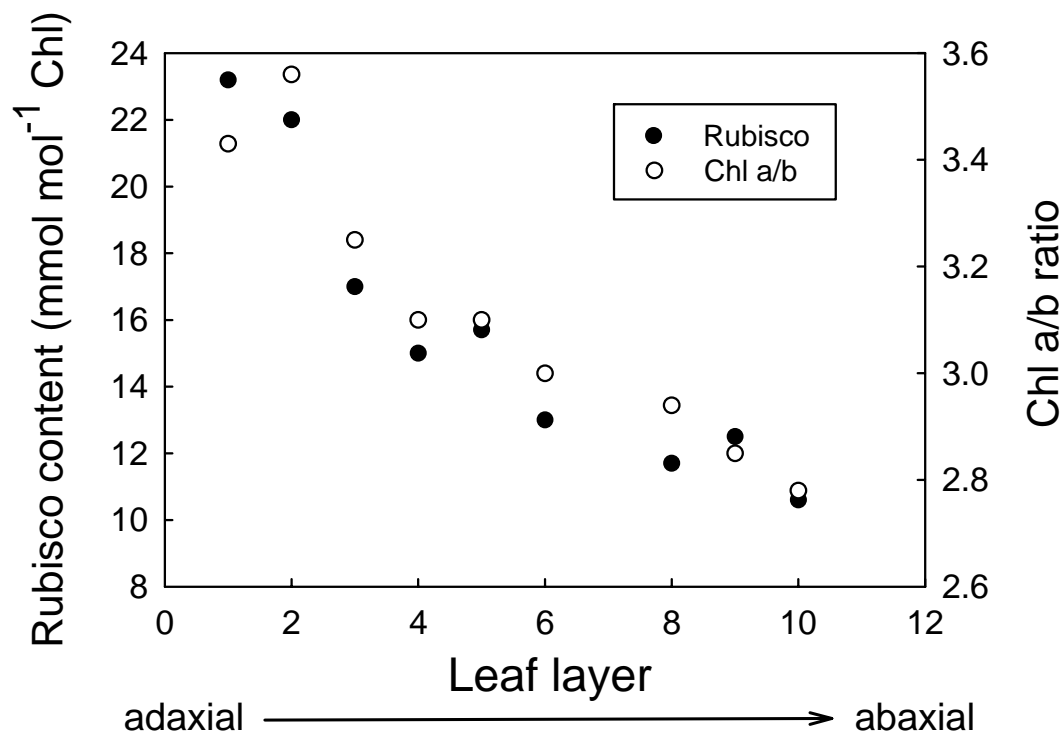


**Figure 6.16.** The decline in Rubisco content and chlorophyll a/b ratio measured in the cells from different vertical layers within a leaf of *Spinacia oleracea* (spinach). Chlorophyll a/b ratio can be used as an index to evaluate photosynthetic adjustment to growth at progressively lower PPFD, with lower Chl a/b occurring in cells acclimated to lower PPFD. Redrawn from Terashima and Inoue (1985).

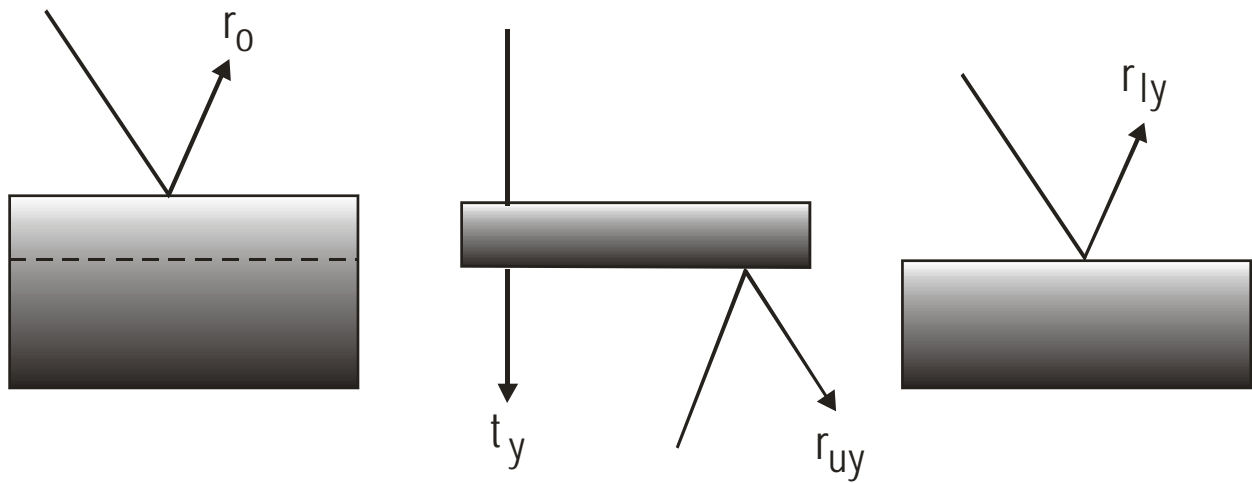


**Figure 6.17.** A diagrammatic definition of the variables used in the model PPF D gradients within leaves developed by Terashima and Saeki (1985). See the text for details of the variables.

**Box 6.1 Specific leaf area: an integrative attribute linking leaf form and function**

The thickness of a leaf is influenced by past selection and subsequent evolution in response to many different environmental forces, and by the environment in which the leaf has developed. Thus, leaf thickness provides an integrative measure of both long-term and short-term influences. Specific leaf area is correlated with rates of leaf metabolism when assessed across broad taxonomic boundaries. As resource limitations (to growth) increase, average specific leaf area decreases (Reich et al. 2003); this is probably due to mutual evolutionary constraints that link specific leaf area and leaf life span. In the face of resource limitation, plant growth may be constrained to the point where short-lived leaves are not sustainable. In environments with significant resource limitation, longer-lived leaves may have a selective advantage. Longer-lived leaves would not only have to be replaced less frequently, they would retain resources within the plant longer; thus, promoting resource conservation. Because they are exposed to the risks of herbivory for a longer life span, however, and because the flow of resources to replace a leaf is slower, longer-lived leaves tend to be more heavily defended with leaf fibers, secondary cell wall thickenings and chemical constituents; this results in tougher, thicker leaves with concomitantly lower specific leaf areas. Thus, in plants native to resource-limited sites, we tend to find a combination of low metabolic capacity, long leaf life span and low specific leaf area. The mutual constraints imposed on each of these attributes through past selection regimes is expressed as positive, quantitative correlations, as we see in the case of leaf photosynthesis rate expressed as a function of specific leaf area when assessed across multiple plant growth forms growing along resource gradients of water and nutrients (Fig. B.6.1.1A). These correlations are useful in modeling studies as they allow us to move along multiple axes of leaf form and function and synthesize dimensional parameters that combine aspects of leaf form and function (e.g., Reich et al. 1997).

While the positive correlation between specific leaf area and leaf net photosynthesis, as seen in Figure B.6.1.1A, is typical of analyses defined by gradients of water and nutrients, we often see the opposite relation when analyses are defined by gradients of light (Fig. B.6.1.1B). In addition to favoring longer leaf life spans, selection in shaded environments favors changes in leaf morphology that enhance photosynthetic photon yield efficiency (i.e., the potential for each unit mass of photosynthetic tissue to convert intercepted photons into net CO<sub>2</sub> assimilation rate). Selection has favored two attributes of leaves that enhance this efficiency. In the first, shade

leaves are constructed with fewer layers of mesophyll cells, compared to sun leaves. This effectively increases the potential to absorb photons per unit of photosynthetic biomass in shade leaves. In the second, shade leaves are constructed with more nitrogen allocated to light harvesting components, such as the chlorophylls associated with photosystem antenna complexes, than to CO<sub>2</sub> harvesting components (such as Rubisco). In a comprehensive modeling analysis, Evans and Poorter (2001) showed that the first attribute – adjustment in the amount of area per unit mass – was most important to the shade tolerance strategy in plants. Thus, the correlation between CO<sub>2</sub> assimilation rate and specific leaf area is negative when assessed across a collection of sun and shade leaves (Fig. B.6.1.1B). From this study, we conclude that selection for enhanced photon use efficiency, and associated lower tissue mass per unit leaf area, in shade leaves is the more dominant selective force, compared to enhanced leaf toughness as a selective covariate with leaf longevity. It should be noted that this pattern of tradeoffs is not always supported by observations. When assessed across broad taxonomic and geographic gradients, some studies have found a positive relation between adaptation to shade and specific leaf area (see Reich et al. 2003, Veneklaas and Poorter 1998). Thus, as the number of species and habitats considered in an analysis increases, the relation between specific leaf area and net photosynthesis rate may converge for light-, water- and nutrient-limited systems. More research will be needed to resolve this issue.

At the more restrictive scale of sun and shade leaves in a single plant, the negative correlation between net photosynthesis rate and specific leaf area is nearly universal. Adjustments in leaf form and function that occur in the same plant (and thus in leaves with the same genetic composition) are referred to as *phenotypic plasticity*, in that the phenotype of the plant has changed but the genotype has remained constant. Phenotypic plasticity is, itself, an adaptive plant attribute, and as such it increases fitness. Sun-shade plasticity provides a means for individual plants to maximize fitness by 'fine-tuning' the cost-benefit ratio of leaves depending on whether they have access to more or less solar energy. The existence of phenotypic plasticity within trees allows us to make logical assumptions about the scaling of net photosynthesis capacity across the vertical space of a canopy. For example, assuming that plasticity has optimized the cost-benefit ratios of leaves across the vertical light gradient of a canopy, we can assume that decreases in the maximum photosynthetic capacity of leaves approximately matches the decrease in mean photon flux density, both as a function of height;

i.e., there should exist a linear relation in the decrease of both variables. This adjustment would be driven principally by phenotypic plasticity in specific leaf area. We will return to this assumption when we discuss ways to linearize canopy photosynthesis models in Chapter 10.

The same type of phenotypic plasticity that controls differential responses in sun and shade leaves within a single plant, are observed to occur within single leaves. Thus, in the palisade (upper) mesophyll cells of a bifacial leaf we tend to observe more mass per unit leaf area and higher allocation of nitrogen to the CO<sub>2</sub> harvesting proteins of photosynthesis, compared to the photon harvesting proteins. The opposite trends are present in the spongy (lower) mesophyll cells, and we assume that this is due to cost-benefit constraints that have emerged during past selection. The vertical gradient in photon flux density that occurs through a single leaf is analogous to the gradient through an entire canopy. Thus, in the same way that we can use patterns of plasticity to assume linearity in the relation between photosynthetic capacities and mean photon flux density across the vertical expanse of a canopy, we can assume linearity in the relations across an individual leaf.

One final issue to consider in the use of correlations such as those shown in Figure B.6.1.1 is that past researchers have expressed net photosynthesis rate in units based on leaf area *or* leaf mass, depending on the analysis. Expression on a leaf area basis is more informative as to the photosynthetic efficiency of energy absorption. Expression on a leaf mass basis is more informative as to the effect of cost-benefit constraints. For example, imagine leaves from two contrasting species, one native to a high-resource environment and one native to a low resource environment. Leaves from the high-resource environment have lower leaf life spans and higher specific leaf area, compared to those from the low-resource environment. Furthermore imagine that the number of mesophyll cells per unit leaf area, and the photosynthetic rate per mesophyll cell, is the same for both leaves, and that the lower specific leaf area in the low-resource leaf is due to greater mass in non-photosynthetic components of the leaf. The photosynthesis rate per unit leaf area would be the same in both leaves, but the photosynthesis rate per unit leaf mass would be lower for the leaf from the low-resource environment. The cost of constructing the low-resource leaf can be best evaluated against the benefits of photosynthetic return if both are expressed on the basis of mass; carbon is assimilated as mass, not area. In contrast, the metric most relevant to studies of plant-atmosphere exchange, is flux density; recall that flux density is defined as flux per unit of cross-sectional area in the direction of the flux (see Section 1.B).

Thus, surface area is the most appropriate means of expressing CO<sub>2</sub> assimilation rate in studies of surface-atmosphere dynamics.

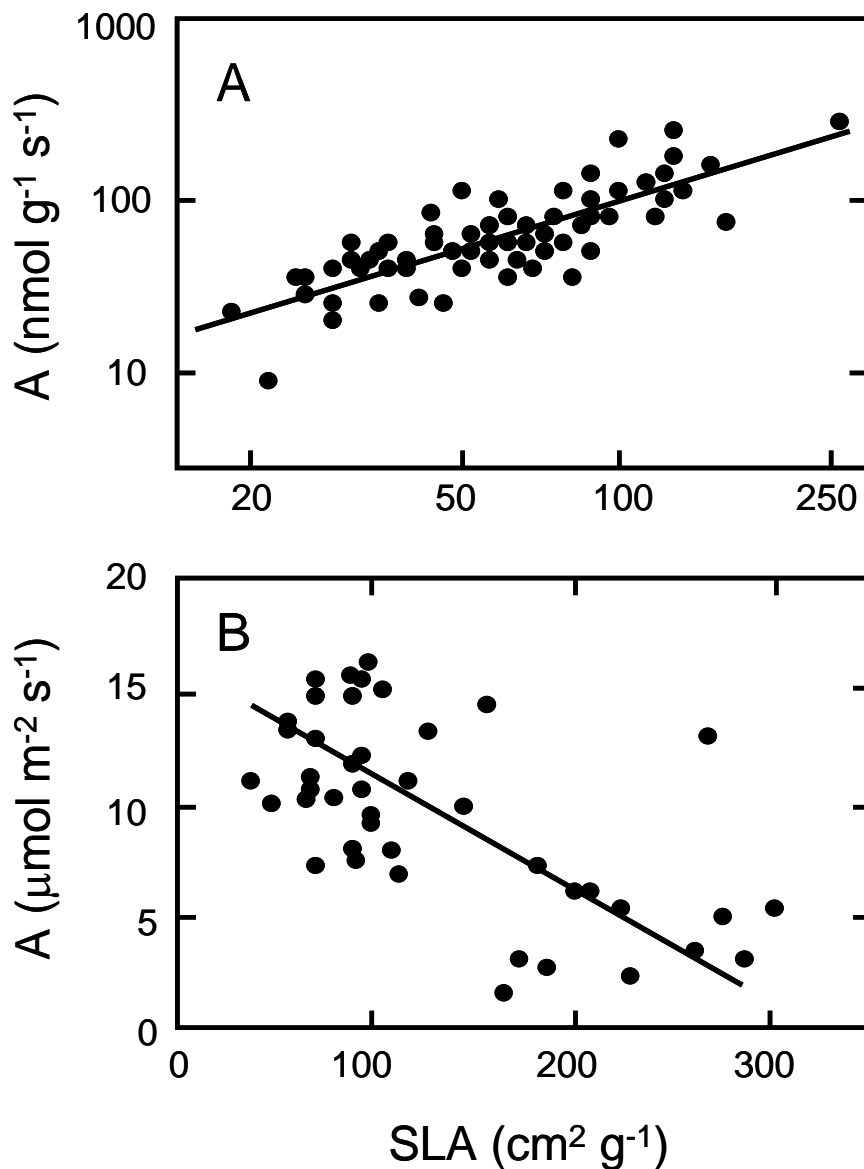


**Figure B.6.1.1.** **A.** Relation between A and SLA among 79 species representing a broad diversity of growth habits growing along an aridity gradient in Australia. **B.** Relation between net CO<sub>2</sub> assimilation rate (A) and specific leaf area (SLA) among 44 different species representing three different growth habits growing in sun and shade habitats of a Panamanian tropical rain forest. Note the logarithmic scales in panel A, and that net CO<sub>2</sub> assimilation rate is expressed on the basis of leaf mass in panel A, but on the basis of leaf area in panel B. Panel A was drawn from data presented in (Wright et al. 2001, 2002 and Reich et al. 2003). Panel B was drawn from data presented in Santiago and Wright (2007).

**Footnotes (Chapter 6):**

<sup>1</sup> The exception to the sun versus shade differentiation of foliage may be found in evergreen, species, in which species adapted to shade environments often have lower specific leaf mass (area per unit mass) (see Lusk et al. 2008).

<sup>2</sup> Direct solar rays are not truly collimated although they can be approximated as such since they have incidence angles within  $1^\circ$  of each other.

<sup>3</sup>  $\tau$  and  $\beta$  may differ significantly from  $t_z$  and  $r_o$ , respectively, due to changes in the diffuse fraction of the photon flux after being reflected from internal leaf surfaces.